SELF-IMPROVING SKILL LEARNING FOR ROBUST SKILL-BASED META-REINFORCEMENT LEARNING

Anonymous authors
Paper under double-blind review

ABSTRACT

Meta-reinforcement learning (Meta-RL) facilitates rapid adaptation to unseen tasks but faces challenges in long-horizon environments. Skill-based approaches tackle this by decomposing state-action sequences into reusable skills and employing hierarchical decision-making. However, these methods are highly susceptible to noisy offline demonstrations, leading to unstable skill learning and degraded performance. To address this, we propose Self-Improving Skill Learning (SISL), which performs self-guided skill refinement using decoupled high-level and skill improvement policies, while applying skill prioritization via maximum return relabeling to focus updates on task-relevant trajectories, resulting in robust and stable adaptation even under noisy and suboptimal data. By mitigating the effect of noise, SISL achieves reliable skill learning and consistently outperforms other skill-based meta-RL methods on diverse long-horizon tasks.

1 INTRODUCTION

Reinforcement Learning (RL) has achieved significant success in domains such as game environments and robotic control (Mnih et al., 2015; Andrychowicz et al., 2020). However, it struggles to adapt quickly to new tasks. Meta-RL addresses this limitation by enabling rapid adaptation to unseen tasks through meta-learning how policies solve problems (Duan et al., 2016; Finn et al., 2017). Among various approaches, context-based meta-RL stands out for its ability to represent similar tasks with analogous contexts and leverage this information in the policy, facilitating quick adaptation to new tasks (Rakelly et al., 2019; Zintgraf et al., 2019). Notably, PEARL (Rakelly et al., 2019) has been widely studied for its high sample efficiency, achieved through off-policy learning, which allows for the reuse of previous samples. Despite these strengths, existing meta-RL methods face challenges in long-horizon environments, where extracting meaningful context information becomes difficult, hindering effective learning.

Skill-based approaches address these challenges by breaking down long state-action sequences into reusable skills, facilitating hierarchical decision-making and enhancing efficiency in complex tasks (Pertsch et al., 2021; 2022; Shi et al., 2023). Among these, SPiRL (Pertsch et al., 2021) defines skills as temporal abstractions of actions, employing them as low-level policies within a hierarchical framework to achieve success in long-horizon tasks. SiMPL (Nam et al., 2022) builds on this by extending skill learning to meta-RL, using offline expert data to train skills and a context-based high-level policy for task-specific skill selection. Despite these advancements, such methods are highly susceptible to noisy offline demonstrations, which can destabilize skill learning and reduce reliability. In real-world settings, noise often stems from factors like infrastructure aging or environmental perturbations, making it crucial to design methods that remain robust under such conditions (Brys et al., 2015; Chae et al., 2022; Yu et al., 2024a).

While noisy demonstration handling has been explored in other RL settings (Sasaki & Yamashina, 2020; Mandlekar et al., 2022), skill-based meta-RL has largely overlooked this challenge. We identify a critical failure mode: when offline data are suboptimal, the skill library becomes corrupted, and this degradation propagates to the high-level policy, ultimately harming adaptation performance. To address this, we propose Self-Improving Skill Learning (SISL), a robust skill-based meta-RL framework with two key contributions: (1) Decoupled skill self-improvement, achieved through a dedicated improvement policy that perturbs trajectories near the offline data distribution, discovers higher-quality rollouts, and supervises its own updates via a prioritized online buffer. This process

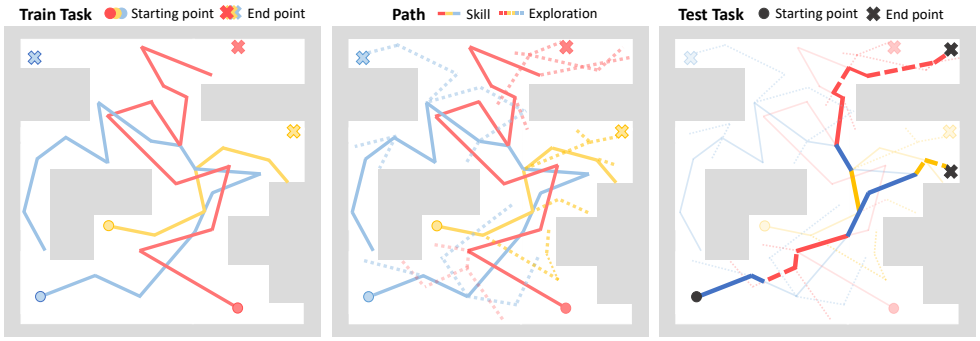

(a) (b) (c)

Figure 1: Sample trajectories in the Maze2D environment: (a) Noisy demonstrations from the offline dataset, (b) Trajectories explored by the exploration policy near the noisy dataset to uncover useful skills, and (c) Trajectories utilizing refined skills to solve unseen test tasks

progressively denoises the skill library while preserving stability. (2) Skill prioritization via maximum return relabeling, which evaluates offline trajectories with a learned reward model, assigns task-relevant hypothetical returns, and reweights them through a softmax prioritization scheme. This suppresses noisy or irrelevant samples and focuses skill updates on the most beneficial trajectories for downstream adaptation. Together, these components dynamically balance offline and online data contributions, yielding a progressively cleaner skill library and accelerating meta-RL convergence. To our knowledge, SISL is the first framework to explicitly address suboptimal demonstrations in skill-based meta-RL through both exploration-guided refinement and principled relabeling, significantly improving robustness and generalization of skill-learning in real-world noisy scenarios.

Fig. 1 illustrates how the proposed algorithm learns effective skills from noisy demonstrations in the Maze2D environment, where the agent starts at a designated point and must reach an endpoint for each task. Fig. 1(a) shows noisy offline trajectories, which fail to produce effective skills when used directly. In contrast, Fig. 1(b) demonstrates how the prioritized refinement framework uses the improvement policy to navigate near noisy trajectories, identifying paths critical for solving long-horizon tasks and refining useful skills through prioritization. Finally, Fig. 1(c) shows how the high-level policy applies these refined skills to successfully solve unseen tasks. These results highlight the method's ability to refine and prioritize skills from noisy datasets, ensuring stable learning and enabling the resolution of long-horizon tasks in unseen environments. This paper is organized as follows: Section 3 provides an overview of meta-RL and skill learning, Section 4 details the proposed framework, and Section 5 presents experimental results showcasing the framework's robustness and effectiveness, along with an ablation study of key components.

2 Related Works

Skill-based Reinforcement Learning: Skill-based RL has gained traction for tackling complex tasks by leveraging temporally extended actions. Researchers have proposed information-theoretic approaches to discover diverse and predictable skills (Gregor et al., 2016; Eysenbach et al., 2018; Achiam et al., 2018; Sharma et al., 2019), with recent work improving skill quality through additional constraints and objectives (Strouse et al., 2022; Park et al., 2022; 2023; Hu et al., 2024). In offline scenarios, approaches focus on learning transferable behavior priors and hierarchical skills from demonstration data (Pertsch et al., 2021; 2022; Shi et al., 2023; Xu et al., 2022; Kipf et al., 2019; Rana et al., 2023). Building upon these foundations, various skill-based meta-RL approaches have been developed, from hierarchical and embedding-based methods (Nam et al., 2022; Chien & Lai, 2023; Cho & Sun, 2024) to task decomposition strategies (Yoo et al., 2022; He et al., 2024) and unsupervised frameworks (Gupta et al., 2018; Jabri et al., 2019; Shin et al., 2024). For clarity, we use skill in the canonical skill-based RL sense: a latent over fixed-length action sequences. Therefore, studies (Yu et al., 2024b; Wu et al.) that lack explicit skill learning are not categorized here.

Relabeling Techniques for Meta-RL: Recent developments in meta-RL have introduced various relabeling techniques to enhance sample efficiency and task generalization (Pong et al., 2022; Jiang et al., 2023). Goal relabeling approaches have extended hindsight experience replay to meta-learning contexts (Packer et al., 2021; Wan et al., 2021), enabling agents to learn from failed attempts. For reward relabeling, model-based approaches have been proposed to relabel experiences across different

tasks (Mendonca et al., 2020), improving adaptation to out-of-distribution scenarios. Beyond these categories, some methods have introduced innovative relabeling strategies using contrastive learning (Yuan & Lu, 2022; Zhou et al., 2024) and metric-based approaches (Li et al., 2020) to create robust task representations in offline settings.

Hierarchical Frameworks: Hierarchical approaches in RL have been pivotal for solving long-horizon tasks, where various methods have been proposed including goal-conditioned learning (Levy et al., 2019; Li et al., 2019; Gehring et al., 2021), and option-based frameworks (Bacon et al., 2017; Riemer et al., 2018; Barreto et al., 2019; Araki et al., 2021). The integration of hierarchical frameworks with meta-RL has shown significant potential for rapid task adaptation and complexity handling (Frans et al., 2018; Fu et al., 2020a; 2023). Recent work has demonstrated that hierarchical architectures in meta-RL can provide theoretical guarantees for learning optimal policies (Chua et al., 2023) and achieve efficient learning through transformer-based architectures (Shala et al., 2024). Recent advances in goal-conditioned RL have focused on improving sample efficiency (Robert et al., 2024), state representation (Yin et al., 2024), and offline-to-online RL (Park et al., 2024; Schmidt et al., 2025). Offline-to-online RL assumes reward-annotated offline datasets to pretrain the policy based on RL before online fine-tuning. In contrast, our setting provides only reward-free offline data for skill learning, making direct application of offline-to-online RL infeasible and clearly distinguishing our approach.

3 BACKGROUND

Meta-Reinforcement Learning Setup: In meta-RL, each task $\mathcal{T}$ is sampled from a distribution $p(\mathcal{T})$ and defined as an MDP environment $\mathcal{M}^{\mathcal{T}} = \big(\mathcal{S}, \mathcal{A}, R^{\mathcal{T}}, P^{\mathcal{T}}, \gamma\big)$, where $\mathcal{S} \times \mathcal{A}$ represents the state-action space, $R^{\mathcal{T}}$ is the reward function, $P^{\mathcal{T}}$ denotes the state transition probability, and γ is the discount factor. At each step t, the agent selects an action a_t via the policy π, receives a reward $r_t := R^{\mathcal{T}}(s_t, a_t)$, and transitions to $s_{t+1} \sim P^{\mathcal{T}}(\cdot|s_t, a_t)$. The goal of meta-RL is to train π to maximize the return $G = \sum_t \gamma^t r_t$ on the training task set $\mathcal{M}_{\text{train}}$ while enabling rapid adaptation to unseen test tasks in $\mathcal{M}_{\text{test}}$, where $\mathcal{M}_{\text{train}} \cap \mathcal{M}_{\text{test}} = \emptyset$.

Offline Dataset and Skill Learning: To address long-horizon tasks, skill learning from an offline dataset $\mathcal{B}_{\text{off}} := \{\tilde{\tau}_{0:H}\}$ is considered, which comprises sample trajectories $\tilde{\tau}_{t:t+k} := (s_t, a_t, \cdots, s_{t+k})$ without reward information, where H is the episode length. The dataset $\mathcal{B}_{\text{off}}$ is typically collected through human interactions or pretrained policies. Among various skill learning methods, SPiRL (Pertsch et al., 2021) focuses on learning a reusable low-level policy π_l, using $q(\cdot|\tilde{\tau}_{t:t+H_s})$ as a skill encoder to extract the skill latent z by minimizing the following loss function:

$$\mathbb{E}_{\substack{\tilde{\tau}_{t:t+H_s} \sim \mathcal{B}_{\text{off}}, \\ z \sim q(\cdot|\tilde{\tau}_{t:t+H_s})}} \left[\mathcal{L}(\pi_l, q, p, z)\right], \tag{1}$$

where $\mathcal{L}(\pi_l, q, p, z) := -\sum_{k=t}^{t+H_s-1} \log \pi_l(a_k|s_k, z) + \lambda_l^{\text{kld}} \mathcal{D}_{\text{KL}}\left(q||\mathcal{N}(\mathbf{0}, \mathbf{I})\right) + \mathcal{D}_{\text{KL}}(\lfloor q \rfloor||p)$, H_s is the skill length, λ_l^{kld} is the coefficient for KL divergence (KLD) $\mathcal{D}_{\text{KL}}$, $\lfloor\cdot\rfloor$ is the stop gradient operator, and $\mathcal{N}(\boldsymbol{\mu}, \boldsymbol{\Sigma})$ represents a Normal distribution with mean $\boldsymbol{\mu}$ and covariance matrix $\mathbf{I}$. Here, $p(z|s_t)$ is the skill prior to obtain the skill distribution z for a given state s_t directly. Using the learned skill policy π_l, the high-level policy π_h is trained within a hierarchical framework using RL methods.

Skill-based Meta-Reinforcement Learning: SiMPL (Nam et al., 2022) integrates skill learning into meta-RL by utilizing an offline dataset of expert demonstrations across various tasks. The skill policy π_l is trained via SPiRL, while a task encoder q_e extracts the task latent $e^{\mathcal{T}} \sim q_e$ using the PEARL (Rakelly et al., 2019) framework, a widely-used meta-RL method. During meta-training, the high-level policy $\pi_h(z|s, e^{\mathcal{T}})$ selects a skill latent z and executes the skill policy $\pi_l(a|s, z)$ for H_s time steps, optimizing π_h to maximize the return for each task $\mathcal{T}$ as:

$$\min_{\pi_h} \mathbb{E}_{\tau_h^{\mathcal{T}} \sim \mathcal{B}_h^{\mathcal{T}}, e^{\mathcal{T}} \sim q_e(\cdot|c^{\mathcal{T}})} \Big[\mathcal{L}_h^{\text{RL}}(\pi_h) + \lambda_h^{\text{kld}} \mathcal{D}_{\text{KL}}\big(\pi_h \,||\, p\big)\Big], \tag{2}$$

where λ_h^{kld} is the KL divergence coefficient, $c^{\mathcal{T}}$ represents the contexts of high-level trajectories $\tau_h^{\mathcal{T}} := (s_0, z_0, \sum_{t=0}^{H_s-1} r_t, s_{H_s}, z_{H_s}, \sum_{t=H_s}^{2H_s-1} r_t, \cdots)$ for task $\mathcal{T}$, $\mathcal{L}_h^{\text{RL}}$ denotes the RL loss for π_h, and $\mathcal{B}_h^{\mathcal{T}} = \{\tau_h^{\mathcal{T}}\}$ is the high-level buffer that stores $\tau_h^{\mathcal{T}}$ for each $\mathcal{T} \in \mathcal{M}_{\text{train}}$. Here, the reward sums $\sum_{t=kH_s}^{(k+1)H_s-1} r_t$ are obtained via environment interactions of $a_t \sim \pi_l(\cdot|s_t, z_{kH_s})$ for $t = kH_s, \cdots, (k+1)H_s - 1$ with $k = 0, \cdots$. During meta-test, the high-level policy is adapted using a limited number of samples, showing good performance on long-horizon tasks.

4 METHODOLOGY

4.1 MOTIVATION: TOWARD ROBUST SKILL LEARNING UNDER NOISY DEMONSTRATIONS

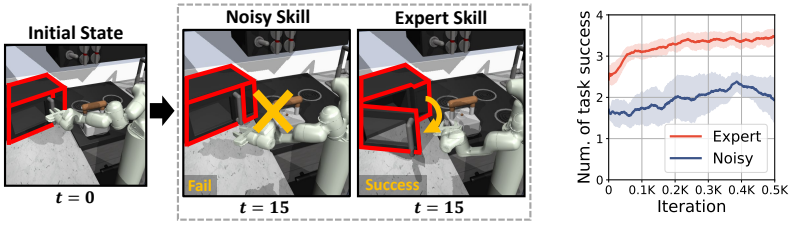

(a) (b)

Figure 2: Comparison of prior skill learning methods in microwave-opening task: (a) Learned skills with expert and noisy demonstrations. (b) Meta-RL performance with the learned skills.

Most existing skill-based meta-RL approaches discussed in Section 3 assume clean offline demonstrations, but real-world datasets are often corrupted by noise from aging hardware, disturbances, or sensor drift. Unlike online training that can adapt through continuous re-training, static offline datasets are particularly susceptible to such noise. This issue becomes critical in long-horizon tasks, where errors accumulate, and in precise manipulation tasks that require reliable execution. Fig. 2(a) illustrates this problem: in the Kitchen microwave-opening task, skills learned from expert demonstrations complete the task successfully, whereas skills learned from noisy data fail even to grasp the handle. This results in a significant downstream performance drop, as shown in Fig. 2(b), where noisy skills lead to poor task success rates and unstable training curves, with each iteration denoting a training loop consisting of policy rollout and update. The root cause is that existing methods treat all trajectories equally, allowing low-quality samples to dominate skill learning.

To address this, we propose the Self-Improving Skill Learning (SISL) framework, which enhances meta-RL by introducing a decoupled skill improvement policy. The high-level policy maximizes returns using the current skill library, while the improvement policy independently perturbs trajectories near the offline data distribution to discover higher-quality variants. The resulting trajectories are selectively stored and prioritized, then used to refine the skill encoder and low-level policy. Through this iterative refinement, SISL progressively denoises the skill library and improves generalization. We further incorporate prioritized buffering and maximum return relabeling as auxiliary mechanisms that enhance sample efficiency and accelerate convergence.

4.2 SELF-IMPROVING SKILL REFINEMENT WITH DECOUPLED POLICIES

We now describe the proposed Self-Improving Skill Learning (SISL) framework, which formalizes the iterative refinement process motivated in Section 4.1. We adopt the standard skill-based meta-RL setup where the skill encoder $q(z|\tilde{\tau}_{t:t+H_s})$ extracts a latent skill z from trajectory segments, the high-level policy $\pi_h(z|s, e^{\mathcal{T}})$ selects z every H_s steps, and the low-level skill policy $\pi_l(a|s, z)$ executes the chosen skill for H_s steps. Building on this setup, SISL decouples training into two complementary components: *a high-level policy* π_h that exploits the current skill library to maximize return, and *a skill-improvement policy* $\pi_{\text{imp}}(a_t|s_t, i)$, defined for each training task $\mathcal{T}_i$ $(i = 1, \ldots, N_{\mathcal{T},\text{train}})$, that deliberately perturbs trajectories near the offline data distribution to discover improved behaviors. This decoupling enables simultaneous exploitation and targeted skill improvement. Perturbations are guided by intrinsic motivation signals (Burda et al., 2018) to encourage coverage of diverse trajectories, although any novelty-driven exploration mechanism could be used. Importantly, unlike generic novelty-driven exploration, π_{imp} restricts perturbations to remain close to the offline data manifold, producing realistic trajectories that can be effectively used to refine π_l. However, when the offline dataset contains noise, training π_{imp} near this distribution in the early stages may be hindered by low-quality samples, reducing the effectiveness of skill improvement.

To overcome this issue, SISL employs a self-supervised guidance mechanism using two additional buffers: The improvement buffer $\mathcal{B}^i_{\text{imp}} = \{\tau^i_{\text{imp}}\}$ stores all trajectories generated by π_{imp}, where each trajectory is $\tau^i_{\text{imp}} = (s^i_0, a^i_0, r^i_0, \ldots, s^i_H)$ with $a^i_t \sim \pi_{\text{imp}}(\cdot|s_t, i)$, and is directly used to update π_{imp} itself, and the prioritized online buffer $\mathcal{B}^i_{\text{on}} = \{\tau^i_{\text{high}}\}$ selectively retains the highest-return trajectories, where each τ^i_{high} is chosen based on its return $G(\tau^i) = \sum_{t=0}^{H-1} \gamma^t r^i_t$. This buffer is initialized with the offline dataset $\mathcal{B}_{\text{off}}$ and gradually becomes dominated by improved trajectories

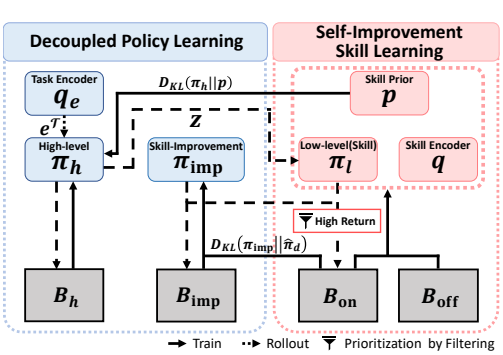

Figure 3: The SISL framework

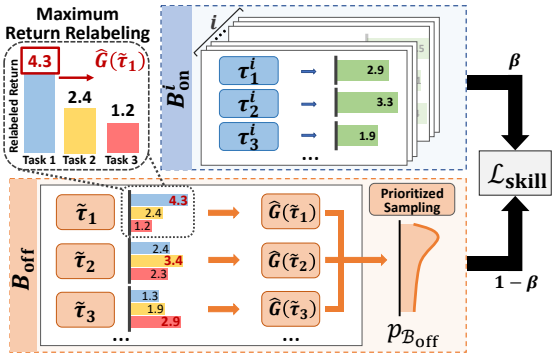

Figure 4: Illustration of maximum return relabeling

generated by both π_{imp} and π_h. This buffer serves two purposes: (1) it provides a cleaner, progressively improving dataset that supervises π_{imp} in a self-supervised manner, guiding it toward regions that have empirically led to success, and (2) it supplies high-quality samples for refining the skill encoder q, skill prior p, and low-level policy π_l.

The skill-improvement policy is then trained so that its trajectory distribution increasingly matches the successful samples in $\mathcal{B}^i_{\text{on}}$ while still exploring variations through controlled perturbations:

$$\sum_i \mathbb{E}_{\tau^i \sim \mathcal{B}^i_{\text{imp}} \cup \mathcal{B}^i_{\text{on}}} \left[\mathcal{L}^{\text{RL}}_{\text{imp}}(\pi_{\text{imp}}) \right] + \lambda^{\text{kld}}_{\text{imp}} \mathbb{E}_{\tau^i \sim \mathcal{B}^i_{\text{on}}} \mathcal{D}_{\text{KL}}(\hat{\pi}^i_d \| \pi_{\text{imp}}), \tag{3}$$

where $\lambda^{\text{kld}}_{\text{imp}}$ is the KLD coefficient and $\hat{\pi}^i_d$ denotes the empirical action distribution derived from $\mathcal{B}^i_{\text{on}}$. $\mathcal{L}^{\text{RL}}_{\text{imp}}$ consists of the standard RL loss combined with intrinsic reward terms for perturbation, with details provided in Appendix B. This loss encourages π_{imp} to iteratively focus on more promising state-action regions discovered so far, effectively turning $\mathcal{B}^i_{\text{on}}$ into a self-improving curriculum that steers exploration away from noisy or uninformative samples.

Building on the improved trajectory distribution obtained from this update, SISL performs skill refinement in dedicated phases every K_{iter} iterations rather than after every update step. At the end of each phase, the skill encoder q, skill prior p, and low-level policy π_l are re-trained on both $\mathcal{B}_{\text{off}}$ and $\mathcal{B}^i_{\text{on}}$ using the SPiRL objective in Eq. 1, and the high-level policy π_h is reinitialized to fully benefit from the updated skill library. This periodic refinement mitigates bias from outdated skill embeddings and accelerates adaptation, as shown in our ablation study in Appendix G.4. These phases yield progressively denoised skills and a stable training signal, enabling π_h to solve tasks more efficiently as training progresses. The overall SISL structure is illustrated in Fig. 3. However, the large number of noisy trajectories in $\mathcal{B}_{\text{off}}$ can still reduce skill learning efficiency. The next section introduces a maximum return relabeling mechanism that prioritizes the most relevant offline trajectories so that only high-value samples significantly influence skill refinement.

4.3 Skill Prioritization via Maximum Return Relabeling

The proposed SISL refines the low-level skills by leveraging both the offline dataset $\mathcal{B}_{\text{off}}$ and the prioritized online buffers $\mathcal{B}^i_{\text{on}}$ for each training task $\mathcal{T}_i$. While $\mathcal{B}^i_{\text{on}}$ provides high-quality trajectories collected from the skill-improvement policy π_{imp} and successful rollouts from π_h, relying solely on it risks overfitting to a narrow distribution and limiting generalization. Conversely, $\mathcal{B}_{\text{off}}$ provides diverse trajectories that are beneficial for generalization but also contains many noisy or suboptimal rollouts, which can degrade skill quality if sampled uniformly. To address this trade-off, we introduce skill prioritization via a *maximum return relabeling* mechanism that assigns hypothetical returns to offline trajectories and reweights samples in both $\mathcal{B}_{\text{off}}$ and $\mathcal{B}^i_{\text{on}}$ according to their estimated task relevance. Specifically, maximum return relabeling assigns each trajectory $\tilde{\tau} \in \mathcal{B}_{\text{off}}$ a hypothetical return that reflects its potential contribution to task success. To compute this return, SISL trains a reward model $\hat{R}(s_t, a_t, i)$ for each task $\mathcal{T}_i$, optimized with the regression loss

$$\mathbb{E}_{(s^i_t, a^i_t, r^i_t) \sim \mathcal{B}^i_{\text{imp}} \cup \mathcal{B}^i_{\text{on}}} \left[(\hat{R}(s^i_t, a^i_t, i) - r^i_t)^2 \right], \tag{4}$$

where the targets r^i_t come from improved trajectories generated by π_{imp} and stored in $\mathcal{B}^i_{\text{on}}$. Since this regression is performed online using actual environment rewards, it remains stable throughout training. Using the trained reward model, SISL computes for each $\tilde{\tau}$ the maximum return

$$\hat{G}(\tilde{\tau}) := \max_i \left\{ \sum_t \gamma^t \hat{R}(s_t, a_t, i) \right\}, \tag{5}$$

which represents the highest predicted cumulative reward across all training tasks. The offline trajectories are then sampled according to a softmax distribution $P_{\mathcal{B}_{\text{off}}}(\tilde{\tau}) = \text{Softmax}\big(\hat{G}(\tilde{\tau})/T\big)$, where $T > 0$ is a temperature parameter controlling prioritization sharpness. This procedure biases sampling toward promising trajectories while suppressing noisy or irrelevant ones, resulting in a cleaner training signal for skill learning. The resulting skill learning objective becomes

$$\mathcal{L}_{\text{skill}}(\pi_l, q, p) := (1-\beta)\mathbb{E}_{\substack{\tilde{\tau}\sim P_{\mathcal{B}_{\text{off}}},\\ z\sim q(\cdot|\tilde{\tau})}}\left[\mathcal{L}(\pi_l, q, p, z)\right] + \frac{\beta}{N_{\mathcal{T},\text{train}}}\sum_i \mathbb{E}_{\substack{\tau^i\sim\mathcal{B}^i_{\text{on}},\\ z\sim q(\cdot|\tau^i)}}\left[\mathcal{L}(\pi_l, q, p, z)\right], \tag{6}$$

where $\mathcal{L}(\pi_l, q, p, z)$ is the SPiRL skill loss defined in Eq. 1. Since $\mathcal{B}_{\text{on}}$ already contains high-return trajectories, samples are drawn uniformly from this buffer. In addtion, the mixing coefficient β is computed dynamically from the offline and online datasets based on their average returns, adaptively balancing their contributions during training as

$$\beta = \frac{\exp(\bar{G}_{\text{on}}/T)}{\exp(\bar{G}_{\text{on}}/T) + \exp(\bar{G}_{\text{off}}/T)}, \tag{7}$$

where $\bar{G}_{\text{off}}$ is the mean $\hat{G}$ across $\mathcal{B}_{\text{off}}$ and $\bar{G}_{\text{on}}$ is the mean return in $\mathcal{B}^i_{\text{on}}$. Fig. 4 illustrates the prioritization process, showing how β dynamically balances contributions from offline and online datasets. This mechanism ensures the selection of task-relevant trajectories from both datasets, facilitating efficient training of the low-level policy. As a result, meta-training yields a refined low-level policy π_l and a high-level policy π_h optimized over progressively cleaner data. During meta-test, π_l is frozen and π_h is adapted to unseen tasks using a small number of interaction trajectories, following the other skill-based meta-RL methods. Additional implementation details for the meta-train and meta-test phases, along with the algorithm table, are provided in Appendix B.

5 Experiment

In this section, we evaluate the robustness of the SISL framework to noisy demonstrations in long-horizon environments and analyze how self-improving skill learning enhance performance.

5.1 Experimental Setup

We compare the proposed SISL with 3 non-meta RL baselines: **SAC**, which trains test tasks directly without using the offline dataset; **SAC+RND**, which incorporates RND-based intrinsic noise for enhanced exploration; and **SPiRL**, which learns skills from the offline dataset using Eq. (1) and trains high-level policies for individual tasks. Also, we include 4 meta-RL baselines: **PEARL**, a widely used context-based meta-RL algorithm without skill learning; **PEARL+RND**, which integrates RND-based exploration into PEARL; **SiMPL**, which applies skill-based meta-RL using Eq. (2); and our **SISL**. SISL's hyperparameters primarily follow Nam et al. (2022), with additional parameters (e.g., temperature T) tuned via hyperparameter search, while other baselines use author-provided code. Results are averaged over 5 random seeds, with standard deviations represented as shaded areas in graphs and $\pm$ values in tables.

5.2 Environmental Setup

(a) Kitchen (b) Office (c) Maze2D (d) AntMaze

Figure 5: Considered long-horizon environments

We evaluate SISL across four long-horizon, multi-task environments: Kitchen and Maze2D from Nam et al. (2022), and Office and AntMaze, newly introduced in this work, as illustrated in Fig. 5. Offline datasets $\mathcal{B}_{\text{off}}$ are generated by perturbing expert policies with varying levels of Gaussian action noise, tailored to each environment. In the Kitchen environment, based on the Franka Kitchen from the D4RL benchmark (Fu et al., 2020b) and proposed by Gupta et al. (2020), a robotic arm completes a sequence of subtasks, with noise levels ranging from expert to $\sigma = 0.1$, 0.2, and 0.3. The Office environment, adapted from Pertsch et al. (2022), involves picking and placing randomly

Table 1: Performance comparison: Final test average return for all considered environments

Environment(Noise)	SAC	SAC+RND	PEARL	PEARL+RND	SPiRL	SiMPL	SISL
Kitchen(Expert)	0.01±0.01	0.02 ±0.05	0.23 ±0.14	0.42±0.16	3.11±0.33	3.40±0.18	**3.97**±0.09
Kitchen($\sigma = 0.1$)					3.37±0.31	3.76±0.14	**3.91**±0.12
Kitchen($\sigma = 0.2$)					2.06±0.43	2.18±0.33	**3.73**±0.16
Kitchen($\sigma = 0.3$)					0.83±0.17	0.81±0.25	**3.48**±0.07
Office(Expert)	0.00±0.00	0.00±0.00	0.01±0.01	0.01±0.01	0.65±0.24	2.50±0.26	**2.86**±0.35
Office($\sigma = 0.1$)					0.91±0.31	3.33±0.39	**3.40**±0.38
Office($\sigma = 0.2$)					0.49±0.22	1.20±0.24	**2.01**±0.24
Office($\sigma = 0.3$)					0.42±0.14	0.11±0.04	**1.68**±0.15
Maze2D(Expert)	0.20±0.06	0.35±0.07	0.10±0.01	0.11±0.08	0.77±0.06	0.80±0.04	**0.87**±0.05
Maze2D($\sigma = 0.5$)					**0.89**±0.03	0.87±0.05	**0.89**±0.03
Maze2D($\sigma = 1.0$)					0.80±0.01	0.87±0.05	**0.93**±0.05
Maze2D($\sigma = 1.5$)					0.81±0.05	0.68±0.06	**0.99**±0.02
AntMaze(Expert)	0.00±0.00	0.00±0.00	0.00±0.00	0.00±0.00	0.64±0.09	0.67±0.07	**0.81**±0.08
AntMaze($\sigma = 0.5$)					0.76±0.10	0.77±0.05	**0.82**±0.05
AntMaze($\sigma = 1.0$)					0.50±0.06	0.33±0.09	**0.60**±0.02
AntMaze($\sigma = 1.5$)					0.30±0.01	0.27±0.05	**0.41**±0.01

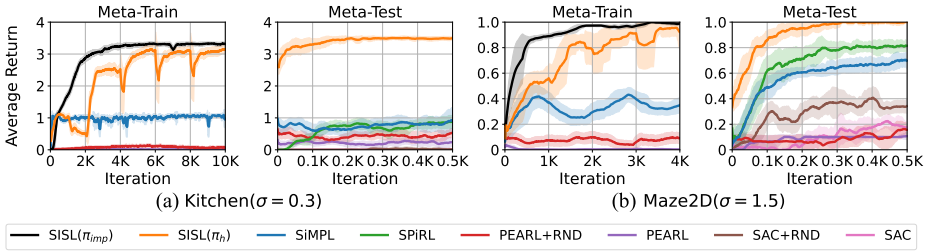

Figure 6: Learning curves of the meta-train and meta-test phases on Kitchen ($\sigma = 0.3$) and Maze2D ($\sigma = 1.5$). SISL (π_{imp}) and SISL (π_h) denote the performance of the skill-improvement policy π_{imp} and high-level policy π_h during meta-training.

selected objects into containers, with Gaussian noise applied at the same levels as Kitchen. Maze2D, based on D4RL (Fu et al., 2020b), requires a point-mass agent to navigate a large 20x20 maze, while AntMaze features a more complex ant agent maneuvering through a 10x10 maze. In both Maze2D and AntMaze, Gaussian noise is introduced at higher levels of $\sigma = 0.5$, 1.0, and 1.5. Each environment is structured with distinct meta-train and meta-test tasks, ensuring that test tasks involve different goals from those seen during training. Further experimental details, including descriptions of other baselines, environment configurations (number of tasks, state representations, and reward setups), initial data collection processes, and hyperparameter settings, are provided in Appendix C.

5.3 Performance Comparison

We compare the proposed SISL with various baseline algorithms. Non-meta RL algorithms are trained directly on each test task for 0.5K iterations due to the absence of a meta-train phase. Meta-RL algorithms undergo meta-training for 10K iterations in Kitchen and Office, and 4K in Maze2D and AntMaze, followed by fine-tuning on test tasks for an additional 0.5K iterations. For SISL, the skill refinement interval K_{iter} is set to 2K for Kitchen, Office, and AntMaze; 1K for Maze2D. To ensure a fair comparison, SISL counts each update process from its skill-improvement policy and high-level policy as one iteration. Table 1 presents the final average return across test tasks after the specified test iterations. The corresponding learning curves are provided in Appendix D.1 for a more detailed comparison. From the result, SAC and PEARL baselines, which do not utilize skills or offline datasets, perform poorly on long-horizon tasks, yielding a single result across all noise levels. In contrast, SPiRL, SiMPL, and SISL, which leverage skills, achieve better performance.

SPiRL and SiMPL, however, show sharp performance declines as dataset noise increases. While both perform well with expert data, SiMPL struggles under noisy conditions due to instability in its task encoder q_e, sometimes performing worse than SPiRL. Here, the baseline results for Maze2D (Expert) are somewhat lower than those reported in the SiMPL paper. This discrepancy likely arises because, in constructing the offline dataset, we considered fewer tasks compared to SiMPL, resulting in trajectories that do not fully cover the map. Interestingly, minor noise occasionally boosts performance by introducing diverse trajectories that improve skill learning, a deteailed analysis of changes in state coverage is provided in Appendix D.1. In contrast, SISL demonstrates superior robustness across all evaluated environments, consistently outperforming baselines at varying noise

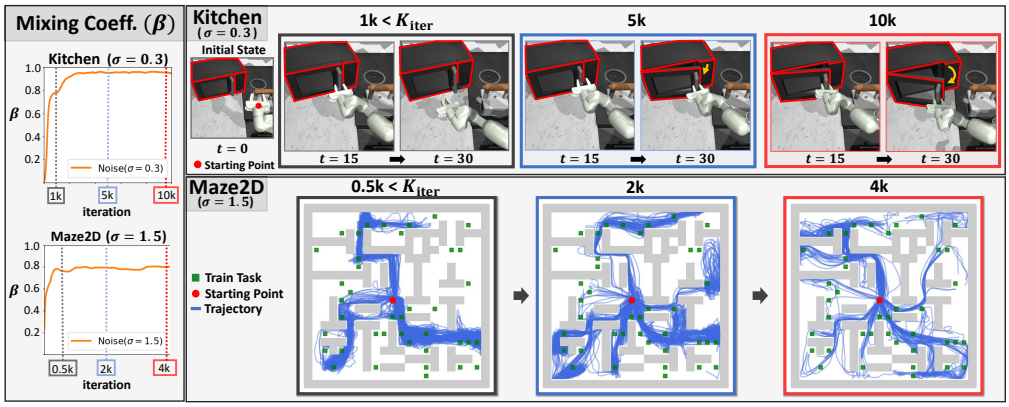

Figure 7: Visualization of buffer mixing coefficient β dynamics and refined skill evolution in Kitchen ($\sigma = 0.3$) and Maze2D ($\sigma = 1.5$). In Kitchen, the refined skills at $t = 15$ and $t = 30$ during the microwave-opening task are depicted, while in Maze2D, trajectories using refined skills illustrate the process of progressively expanding to broader areas to solve tasks.

levels. For example, in the Kitchen environment, SISL maintains strong performance under significant noise by effectively refining useful skills, while in Maze2D, higher noise levels lead to the improvement of diverse skills, achieving perfect task completion when $\sigma = 1.5$. These results highlight SISL's ability to discover improved behavior and refine robust skills, significantly enhancing meta-RL performance. Moreover, SISL excels with both noisy and expert data, achieving superior test performance by learning more effective skills.

Fig. 6 shows the learning progress during the meta-train/test phases for Kitchen ($\sigma = 0.3$) and Maze2D ($\sigma = 1.5$), highlighting the performance gap between SISL and other methods. The periodic drops in SISL's high-level performance correspond to the reinitialization of π_h every K_{iter}. Non-meta RL algorithms, including those with RND-based exploration, struggle with long-horizon tasks, while SPiRL and SiMPL show limited improvement due to their reliance on noisy offline datasets. In contrast, SISL's self-improving skill refinement supports continuous skill improvement, resulting in superior meta-test performance. To further assess SISL's robustness, we perform experiments with limited offline data, random noise injection, and diverse sub-optimal datasets in Appendix D, reflecting real-world challenges such as costly data collection and unstructured anomalies. Even under these conditions, SISL consistently outperforms the baselines, demonstrating strong robustness. Furthermore, we provide a computational cost analysis with SiMPL in Appendix E, and the result shows that SISL requires about 16% more computation time per iteration during meta-training, while the meta-test phase remains unchanged. Notably, even with extended training, SiMPL fails to achieve further performance gains, highlighting SISL's advantage.

5.4 In-depth Analysis of the Proposed Skill Refinement Process

To analyze skill refinement and prioritization in more detail, Fig. 7 illustrates the evolution of the buffer mixing coefficient β and skill refinement in Kitchen ($\sigma = 0.3$) and Maze2D ($\sigma = 1.5$). For Kitchen, the microwave-opening subtask is evaluated, while Maze2D focuses on navigation improvements. In the early stages (1K iterations for Kitchen, 0.5K for Maze2D), pretrained skills from the offline dataset are used without updates, resulting in poor performance, with the agent failing to grasp the handle in Kitchen and producing noisy trajectories in Maze2D. As training progresses, β increases to shift contribution from offline data to newly collected high-quality data, providing task-relevant refinement. By design, the increase of β tracks task-return improvement and serves as a soft curriculum that prevents abrupt distribution shift. At the same time, prioritized offline samples keep β below 1, thereby ensuring generalization.

As a result, by iteration 5K in Kitchen, the agent learns to open the microwave, refining this skill to complete the task more efficiently by iteration 10K. In Maze2D, the agent explores more diverse trajectories over iterations, ultimately solving all training tasks by iteration 4K. These results highlight how SISL refines skills iteratively by leveraging prioritized data from offline and online buffers. As shown in Table 1, the learned skills generalize effectively to unseen test tasks, demonstrating SISL's robustness and efficacy. While variations in return scales across tasks can introduce bias in reward model training, our experimental environments adopt a simple reward structure based on subtask

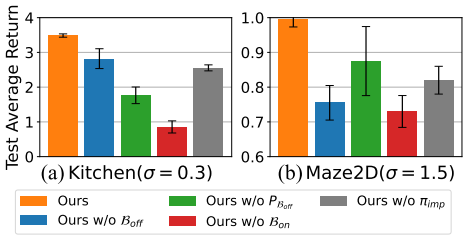

Figure 8: Component evaluation

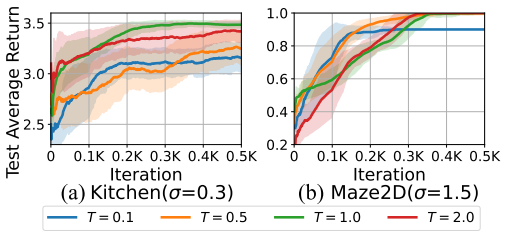

Figure 9: Impact of prioritization temperature T

completion, under which the reward model remains stable, as shown in Appendix F.4. For environments with more complex reward functions, per-task reward standardization can be considered. We provide β trends and visualize refined skills, task-representation improvements, and policy skill composition in Appendix F. These analyses provide insights into SISL's effectiveness in optimizing skill execution and enhancing task representation.

5.5 Ablation Studies

We evaluate the impact of SISL's components and key hyperparameters in Kitchen ($\sigma = 0.3$) and Maze2D ($\sigma = 1.5$), focusing on the effect of the prioritization temperature T. Additional analyses, including component evaluation and KLD coefficient $\lambda_{\text{imp}}^{\text{kld}}$ for all noise levels, are in Appendix G.

Component Evaluation: To evaluate the importance of SISL's components, we compare the meta-test performance of SISL with all components included against the following variations: (1) Without $\mathcal{B}_{\text{off}}$, relying solely on $\mathcal{B}_{\text{on}}^{i}$, to evaluate the influence of offline data in skill refinement; (2) Without $P_{\mathcal{B}_{\text{off}}}$, applying uniform sampling in $\mathcal{B}_{\text{off}}$ instead of maximum return relabeling, to evaluate the effect of prioritization; (3) Without $\mathcal{B}_{\text{on}}$, using only $\mathcal{B}_{\text{off}}$, to evaluate the contribution of high-quality samples obtained by π_{imp} and π_h; and (4) Without π_{imp}, removing the skill-improvement policy, to evaluate whether exploration near the skill distribution discovers improved behaviors. Fig. 8 presents the comparison results, demonstrating significant performance drops when either buffer is removed, highlighting their critical role in effective skill discovery. Uniform sampling in $\mathcal{B}_{\text{off}}$ also reduces performance, underlining the importance of maximum return relabeling. Lastly, excluding π_{imp} notably degrades performance, emphasizing the critical role of discovering improved behavior.

Prioritization Temperature T: The prioritization temperature T adjusts the prioritization between online and offline buffers. Specifically, lower T biases sampling toward high-return buffers, while higher T results in uniform sampling. Fig. 9 illustrates the performance variations with different prioritization temperatures T. When $T = 0.1$, performance degrades due to excessive focus on a single buffer, aligning with the trends observed in the component evaluation. Conversely, high $T = 2.0$ also degrades performance by eliminating prioritization. These results highlight the importance of proper tuning: $T = 1.0$ for Kitchen and $T = 0.5$ for Maze2D achieve the best performance. Based on the result, we set T approximately proportional to the high-return range of each environment, which consistently yielded the best performance while avoiding extensive tuning.

6 Limitation

Although SISL demonstrates strong performance, it has several limitations. First, although SISL achieves notable performance gains, its computation time per iteration increases by 16% over the baseline. This overhead mainly comes from training the skill model without freezing it during meta-training, but the performance table and ablation study confirm that this component is essential. (See Appendix E for details) Second, SISL requires fine-tuning during the meta-test phase for optimal performance, which introduces additional computational overhead. Addressing this through zero-shot skill adaptation could enhance its practicality, enabling transfer to new tasks without retraining. Future work in this direction could significantly improve SISL's applicability in real-world scenarios.

7 Conclusion

In this paper, we propose SISL, a robust skill-based meta-RL framework designed to address noisy offline demonstrations in long-horizon tasks. Through self-improving skill refinement and prioritization via maximum return relabeling, SISL effectively prioritizes task-relevant trajectories for skill learning and enabling efficient exploration and targeted skill optimization. Experimental results highlight its robustness to noise and superior performance across various environments, demonstrating its potential for scalable meta-RL in real-world applications where data quality is critical.

ETHICS STATEMENT

By introducing self-improving skill refinement and skill prioritization via maximum return relabeling, SISL improves the stability and generalizability of skill learning, allowing agents to adapt rapidly to new tasks even when data quality is imperfect. This advancement has the potential to make reinforcement learning more practical and reliable in real-world settings where collecting high-quality data is difficult or expensive. While this framework may have potential societal implications by enhancing reinforcement learning's real-world applicability, we believe it is primarily foundational in nature and does not introduce any new risks of malicious use.

REPRODUCIBILITY STATEMENT

To reproduce SISL, we provide the loss function redefined as neural network parameters, along with the meta-train and meta-test algorithm tables in Appendix B. For the algorithm implementation, we provide the system specifications used for experiments, the source of the baseline algorithm, environment details, the offline dataset construction method, and the hyperparameter setup in Appendix C. Additionally, we provide the anonymized code for SISL in the supplementary material, enabling the reproduction of the proposed algorithm and experiment results.

REFERENCES

Joshua Achiam, Harrison Edwards, Dario Amodei, and Pieter Abbeel. Variational option discovery algorithms. *arXiv preprint arXiv:1807.10299*, 2018.

OpenAI: Marcin Andrychowicz, Bowen Baker, Maciek Chociej, Rafal Jozefowicz, Bob McGrew, Jakub Pachocki, Arthur Petron, Matthias Plappert, Glenn Powell, Alex Ray, et al. Learning dexterous in-hand manipulation. *The International Journal of Robotics Research*, 39:3–20, 2020.

Brandon Araki, Xiao Li, Kiran Vodrahalli, Jonathan DeCastro, Micah Fry, and Daniela Rus. The logical options framework. In *International Conference on Machine Learning*, pp. 307–317. PMLR, 2021.

Pierre-Luc Bacon, Jean Harb, and Doina Precup. The option-critic architecture. In *Proceedings of the AAAI conference on artificial intelligence*, volume 31, 2017.

André Barreto, Diana Borsa, Shaobo Hou, Gheorghe Comanici, Eser Aygün, Philippe Hamel, Daniel Toyama, Shibl Mourad, David Silver, Doina Precup, et al. The option keyboard: Combining skills in reinforcement learning. *Advances in Neural Information Processing Systems*, 32, 2019.

Tim Brys, Anna Harutyunyan, Halit Bener Suay, Sonia Chernova, Matthew E Taylor, and Ann Nowé. Reinforcement learning from demonstration through shaping. In *Twenty-fourth international joint conference on artificial intelligence*, 2015.

Yuri Burda, Harrison Edwards, Amos Storkey, and Oleg Klimov. Exploration by random network distillation. In *International Conference on Learning Representations*, 2018.

Jongseong Chae, Seungyul Han, Whiyoung Jung, Myungsik Cho, Sungho Choi, and Youngchul Sung. Robust imitation learning against variations in environment dynamics. In *International Conference on Machine Learning*, pp. 2828–2852. PMLR, 2022.

Jen-Tzung Chien and Weiwei Lai. Variational skill embeddings for meta reinforcement learning. In *2023 International Joint Conference on Neural Networks (IJCNN)*, pp. 1–8. IEEE, 2023.

Minjae Cho and Chuangchuang Sun. Hierarchical meta-reinforcement learning via automated macro-action discovery. *arXiv preprint arXiv:2412.11930*, 2024.

Kurtland Chua, Qi Lei, and Jason Lee. Provable hierarchy-based meta-reinforcement learning. In *International Conference on Artificial Intelligence and Statistics*, pp. 10918–10967. PMLR, 2023.

Yan Duan, John Schulman, Xi Chen, Peter L Bartlett, Ilya Sutskever, and Pieter Abbeel. Rl^2: Fast reinforcement learning via slow reinforcement learning. *arXiv preprint arXiv:1611.02779*, 2016.

Benjamin Eysenbach, Abhishek Gupta, Julian Ibarz, and Sergey Levine. Diversity is all you need: Learning skills without a reward function. In *International Conference on Learning Representations*, 2018.

Chelsea Finn, Pieter Abbeel, and Sergey Levine. Model-agnostic meta-learning for fast adaptation of deep networks. In *International conference on machine learning*, pp. 1126–1135. PMLR, 2017.

Kevin Frans, Jonathan Ho, Xi Chen, Pieter Abbeel, and John Schulman. Meta learning shared hierarchies. In *International Conference on Learning Representations*, 2018.

Haotian Fu, Hongyao Tang, Jianye Hao, Wulong Liu, and Chen Chen. Mghrl: Meta goal-generation for hierarchical reinforcement learning. In *Distributed Artificial Intelligence: Second International Conference, DAI 2020, Nanjing, China, October 24–27, 2020, Proceedings 2*, pp. 29–39. Springer, 2020a.

Haotian Fu, Shangqun Yu, Saket Tiwari, Michael Littman, and George Konidaris. Meta-learning parameterized skills. In *Proceedings of the 40th International Conference on Machine Learning*, pp. 10461–10481, 2023.

Justin Fu, Aviral Kumar, Ofir Nachum, George Tucker, and Sergey Levine. D4rl: Datasets for deep data-driven reinforcement learning. *arXiv preprint arXiv:2004.07219*, 2020b.

Jonas Gehring, Gabriel Synnaeve, Andreas Krause, and Nicolas Usunier. Hierarchical skills for efficient exploration. *Advances in Neural Information Processing Systems*, 34:11553–11564, 2021.

Alex Graves and Alex Graves. Long short-term memory. *Supervised sequence labelling with recurrent neural networks*, pp. 37–45, 2012.

Karol Gregor, Danilo Jimenez Rezende, and Daan Wierstra. Variational intrinsic control. *arXiv preprint arXiv:1611.07507*, 2016.

Abhishek Gupta, Benjamin Eysenbach, Chelsea Finn, and Sergey Levine. Unsupervised meta-learning for reinforcement learning. *arXiv preprint arXiv:1806.04640*, 2018.

Abhishek Gupta, Vikash Kumar, Corey Lynch, Sergey Levine, and Karol Hausman. Relay policy learning: Solving long-horizon tasks via imitation and reinforcement learning. In *Conference on Robot Learning*, pp. 1025–1037. PMLR, 2020.

Tuomas Haarnoja, Aurick Zhou, Pieter Abbeel, and Sergey Levine. Soft actor-critic: Off-policy maximum entropy deep reinforcement learning with a stochastic actor. In *International conference on machine learning*, pp. 1861–1870. PMLR, 2018.

Hongcai He, Anjie Zhu, Shuang Liang, Feiyu Chen, and Jie Shao. Decoupling meta-reinforcement learning with gaussian task contexts and skills. In *Proceedings of the AAAI Conference on Artificial Intelligence*, volume 38, pp. 12358–12366, 2024.

Jiaheng Hu, Zizhao Wang, Peter Stone, and Roberto Martín-Martín. Disentangled unsupervised skill discovery for efficient hierarchical reinforcement learning. In *The Thirty-eighth Annual Conference on Neural Information Processing Systems*, 2024.

Allan Jabri, Kyle Hsu, Abhishek Gupta, Ben Eysenbach, Sergey Levine, and Chelsea Finn. Unsupervised curricula for visual meta-reinforcement learning. *Advances in Neural Information Processing Systems*, 32, 2019.

Yuankun Jiang, Nuowen Kan, Chenglin Li, Wenrui Dai, Junni Zou, and Hongkai Xiong. Doubly robust augmented transfer for meta-reinforcement learning. *Advances in Neural Information Processing Systems*, 36:77002–77012, 2023.

Woojun Kim, Yongjae Shin, Jongeui Park, and Youngchul Sung. Sample-efficient and safe deep reinforcement learning via reset deep ensemble agents. *Advances in neural information processing systems*, 36:53239–53260, 2023.

Thomas Kipf, Yujia Li, Hanjun Dai, Vinicius Zambaldi, Alvaro Sanchez-Gonzalez, Edward Grefenstette, Pushmeet Kohli, and Peter Battaglia. Compile: Compositional imitation learning and execution. In *International Conference on Machine Learning*, pp. 3418–3428. PMLR, 2019.

Rui Kong, Chenyang Wu, Chen-Xiao Gao, Zongzhang Zhang, and Ming Li. Efficient and stable offline-to-online reinforcement learning via continual policy revitalization. In *Proceedings of the Thirty-Third International Joint Conference on Artificial Intelligence, IJCAI-24*, pp. 4317–4325, 2024.

Juho Lee, Yoonho Lee, Jungtaek Kim, Adam Kosiorek, Seungjin Choi, and Yee Whye Teh. Set transformer: A framework for attention-based permutation-invariant neural networks. In *International conference on machine learning*, pp. 3744–3753. PMLR, 2019.

Andrew Levy, George Konidaris, Robert Platt, and Kate Saenko. Learning multi-level hierarchies with hindsight. In *Proceedings of International Conference on Learning Representations*, 2019.

Jiachen Li, Quan Vuong, Shuang Liu, Minghua Liu, Kamil Ciosek, Henrik Christensen, and Hao Su. Multi-task batch reinforcement learning with metric learning. *Advances in neural information processing systems*, 33:6197–6210, 2020.

Siyuan Li, Rui Wang, Minxue Tang, and Chongjie Zhang. Hierarchical reinforcement learning with advantage-based auxiliary rewards. *Advances in Neural Information Processing Systems*, 32, 2019.

Ajay Mandlekar, Danfei Xu, Josiah Wong, Soroush Nasiriany, Chen Wang, Rohun Kulkarni, Li Fei-Fei, Silvio Savarese, Yuke Zhu, and Roberto Martín-Martín. What matters in learning from offline human demonstrations for robot manipulation. In *Conference on Robot Learning*, pp. 1678–1690. PMLR, 2022.

Russell Mendonca, Xinyang Geng, Chelsea Finn, and Sergey Levine. Meta-reinforcement learning robust to distributional shift via model identification and experience relabeling. *arXiv preprint arXiv:2006.07178*, 2020.

Volodymyr Mnih, Koray Kavukcuoglu, David Silver, Andrei A Rusu, Joel Veness, Marc G Bellemare, Alex Graves, Martin Riedmiller, Andreas K Fidjeland, Georg Ostrovski, et al. Human-level control through deep reinforcement learning. *nature*, 518:529–533, 2015.

Taewook Nam, Shao-Hua Sun, Karl Pertsch, Sung Ju Hwang, and Joseph J. Lim. Skill-based meta-reinforcement learning. In *International Conference on Learning Representations (ICLR)*, 2022.

Charles Packer, Pieter Abbeel, and Joseph E Gonzalez. Hindsight task relabelling: Experience replay for sparse reward meta-rl. *Advances in neural information processing systems*, 34:2466–2477, 2021.

Seohong Park, Jongwook Choi, Jaekyeom Kim, Honglak Lee, and Gunhee Kim. Lipschitz-constrained unsupervised skill discovery. In *International Conference on Learning Representations*, 2022.

Seohong Park, Kimin Lee, Youngwoon Lee, and Pieter Abbeel. Controllability-aware unsupervised skill discovery. In *International Conference on Machine Learning*, pp. 27225–27245. PMLR, 2023.

Seohong Park, Dibya Ghosh, Benjamin Eysenbach, and Sergey Levine. Hiql: Offline goal-conditioned rl with latent states as actions. *Advances in Neural Information Processing Systems*, 36, 2024.

Karl Pertsch, Youngwoon Lee, and Joseph Lim. Accelerating reinforcement learning with learned skill priors. In *Conference on robot learning*, pp. 188–204. PMLR, 2021.

Karl Pertsch, Youngwoon Lee, Yue Wu, and Joseph J Lim. Guided reinforcement learning with learned skills. In *Conference on Robot Learning*, pp. 729–739. PMLR, 2022.

Vitchyr H Pong, Ashvin V Nair, Laura M Smith, Catherine Huang, and Sergey Levine. Offline meta-reinforcement learning with online self-supervision. In *International Conference on Machine Learning*, pp. 17811–17829. PMLR, 2022.

Kate Rakelly, Aurick Zhou, Chelsea Finn, Sergey Levine, and Deirdre Quillen. Efficient off-policy meta-reinforcement learning via probabilistic context variables. In *International conference on machine learning*, pp. 5331–5340. PMLR, 2019.

Krishan Rana, Ming Xu, Brendan Tidd, Michael Milford, and Niko Sünderhauf. Residual skill policies: Learning an adaptable skill-based action space for reinforcement learning for robotics. In *Conference on Robot Learning*, pp. 2095–2104. PMLR, 2023.

Matthew Riemer, Miao Liu, and Gerald Tesauro. Learning abstract options. *Advances in neural information processing systems*, 31, 2018.

Arnaud Robert, Ciara Pike-Burke, and Aldo A Faisal. Sample complexity of goal-conditioned hierarchical reinforcement learning. *Advances in Neural Information Processing Systems*, 36, 2024.

Fumihiro Sasaki and Ryota Yamashina. Behavioral cloning from noisy demonstrations. In *International Conference on Learning Representations*, 2020.

Carolin Schmidt, Daniele Gammelli, James Harrison, Marco Pavone, and Filipe Rodrigues. Offline hierarchical reinforcement learning via inverse optimization. In *The Thirteenth International Conference on Learning Representations*, 2025.

Gresa Shala, André Biedenkapp, and Josif Grabocka. Hierarchical transformers are efficient meta-reinforcement learners. *arXiv preprint arXiv:2402.06402*, 2024.

Archit Sharma, Shixiang Gu, Sergey Levine, Vikash Kumar, and Karol Hausman. Dynamics-aware unsupervised discovery of skills. In *International Conference on Learning Representations*, 2019.

Lucy Xiaoyang Shi, Joseph J Lim, and Youngwoon Lee. Skill-based model-based reinforcement learning. In *Conference on Robot Learning*, pp. 2262–2272. PMLR, 2023.

Sangwoo Shin, Minjong Yoo, Jeongwoo Lee, and Honguk Woo. Semtra: A semantic skill translator for cross-domain zero-shot policy adaptation. In *Proceedings of the AAAI Conference on Artificial Intelligence*, volume 38, pp. 15000–15008, 2024.

DJ Strouse, Kate Baumli, David Warde-Farley, Volodymyr Mnih, and Steven Stenberg Hansen. Learning more skills through optimistic exploration. In *International Conference on Learning Representations*, 2022.

Michael Wan, Jian Peng, and Tanmay Gangwani. Hindsight foresight relabeling for meta-reinforcement learning. In *International Conference on Learning Representations*, 2021.

Te-Lin Wu, Jaedong Hwang, Jingyun Yang, Shaofan Lai, Carl Vondrick, and Joseph J Lim. Learning from noisy demonstration sets via meta-learned suitability assessor.

Mengda Xu, Manuela Veloso, and Shuran Song. Aspire: Adaptive skill priors for reinforcement learning. *Advances in Neural Information Processing Systems*, 35:38600–38613, 2022.

Xiangyu Yin, Sihao Wu, Jiaxu Liu, Meng Fang, Xingyu Zhao, Xiaowei Huang, and Wenjie Ruan. Representation-based robustness in goal-conditioned reinforcement learning. In *Proceedings of the AAAI Conference on Artificial Intelligence*, volume 38, pp. 21761–21769, 2024.

Minjong Yoo, Sangwoo Cho, and Honguk Woo. Skills regularized task decomposition for multi-task offline reinforcement learning. *Advances in Neural Information Processing Systems*, 35: 37432–37444, 2022.

Xingrui Yu, Bo Han, and Ivor W Tsang. Usn: A robust imitation learning method against diverse action noise. *Journal of Artificial Intelligence Research*, 79:1237–1280, 2024a.

Xuehui Yu, Mhairi Dunion, Xin Li, and Stefano V Albrecht. Skill-aware mutual information optimisation for zero-shot generalisation in reinforcement learning. *Advances in Neural Information Processing Systems*, 37:110573–110612, 2024b.

Haoqi Yuan and Zongqing Lu. Robust task representations for offline meta-reinforcement learning via contrastive learning. In *International Conference on Machine Learning*, pp. 25747–25759. PMLR, 2022.

Renzhe Zhou, Chen-Xiao Gao, Zongzhang Zhang, and Yang Yu. Generalizable task representation learning for offline meta-reinforcement learning with data limitations. In *Proceedings of the AAAI Conference on Artificial Intelligence*, volume 38, pp. 17132–17140, 2024.

Luisa Zintgraf, Kyriacos Shiarlis, Maximilian Igl, Sebastian Schulze, Yarin Gal, Katja Hofmann, and Shimon Whiteson. Varibad: A very good method for bayes-adaptive deep rl via meta-learning. In *International Conference on Learning Representations*, 2019.

A THE USE OF LARGE LANGUAGE MODELS (LLMS)

We wrote the entire manuscript ourselves, including the main text and the appendix. We used large language models only for copy editing to improve spelling and readability, and we verified all suggested revisions before incorporation. LLMs were not used to generate ideas, methods, analyses, results, code, figures, or citations beyond minor edits. All technical content and experiments were conceived, implemented, and validated by the authors. We manually audited every citation and numerical claim and accept full responsibility for the manuscript.

B IMPLEMENTATION DETAILS ON SISL

This section provides a detailed implementation of the proposed SISL framework. As outlined in Section 4, SISL begins with an initial skill learning phase (pre-train) to train the low-level skill policy, skill encoder, and skill prior. It then progresses to the meta-train phase, where **decoupled policy learning** is performed using high-level policy, task encoder, and skill-improvement policy. Also, **self-improvement skill learning** is executed via maximum return relabeling using reward model, low-level skill policy, skill encoder, and skill prior. Finally, in the meta-test phase, rapid adaptation to the target task is achieved via fine-tuning based on the trained high-level policy and task encoder. Section B.1 details the initial skill learning phase, Section B.2 elaborates on the meta-train phase, and Section B.3 explains the meta-test phase. All loss functions in SISL are redefined in terms of the neural network parameters of its policies and models. Additionally, the overall structure for the meta-train and meta-test phases is provided in Algorithms 1 and 2.

B.1 INITIAL SKILL LEARNING PHASE

Following SPiRL (Pertsch et al., 2021), introduced in Section 3, we train initial skills using the offline dataset $\mathcal{B}_{\text{off}}$. The low-level skill policy $\pi_{l,\phi}$, skill encoder q_ϕ, and skill prior p_ϕ are parameterized by ϕ and trained using the following loss function (modified from Eq. (1)):

$$
\begin{aligned}
&\mathcal{L}_{\text{spirl}}(\phi) \\
&:= \mathbb{E}_{\substack{(s_{t:t+H_s}, a_{t:t+H_s}) \sim \mathcal{B}_{\text{off}} \\ z \sim q_\phi(\cdot | s_{t:t+H_s}, a_{t:t+H_s})}} \Big[\mathcal{L}(\pi_{l,\phi}, q_\phi, p_\phi, z) \Big] \\
&= \mathbb{E}_{\substack{(s_{t:t+H_s}, a_{t:t+H_s}) \sim \mathcal{B}_{\text{off}} \\ z \sim q_\phi(\cdot | s_{t:t+H_s}, a_{t:t+H_s})}} \Bigg[- \sum_{k=t}^{t+H_s-1} \log \pi_{l,\phi}(a_k | s_k, z) + \lambda_l^{\text{kld}} \mathcal{D}_{\text{KL}} \Big(q_\phi(\cdot | s_{t:t+H_s}, a_{t:t+H_s}) \,\Big\|\, \mathcal{N}(\mathbf{0}, \mathbf{I}) \Big) \\
&\qquad\qquad + \mathcal{D}_{\text{KL}} \Big(\lfloor q_\phi(\cdot | s_{t:t+H_s}, a_{t:t+H_s}) \rfloor \,\Big\|\, p_\phi(\cdot | s_t) \Big) \Bigg],
\end{aligned}
\tag{B.1}
$$

where $\lfloor \cdot \rfloor$ represents the stop gradient operator, which prevents the KL term for skill prior learning from influencing the skill encoder. Using the pre-trained $\pi_{l,\phi}$, q_ϕ, and p_ϕ, SISL refines skills during the meta-train phase to further enhance task-solving capabilities.

B.2 META-TRAIN PHASE

As described in Section 4, SISL comprises two main processes: **Decoupled Policy Learning**, which explores task-relevant behavior near skill distribution using skill-improvement policy, and trains the high-level policy, task encoder to effectively utilize learned skills for solving tasks; and **Self-Improvement Skill Learning**, which improves skills using prioritization via maximum return relabeling. Detailed explanations for each process are provided below.

Decoupled Policy Learning

As described in Section 4.2, the skill-improvement policy $\pi_{\text{imp},\psi}$, parameterized by ψ, is designed to expand the skill distribution and discover task-relevant behaviors near trajectories stored in the prioritized on-policy buffer $\mathcal{B}_{\text{on}}^i$ for each training task $\mathcal{T}^i$. This buffer prioritizes trajectories that best solve the tasks. Additionally, the state-action value function $Q_{\text{imp},\psi}$, also parameterized by ψ, is defined to train the skill-improvement policy using soft actor-critic (SAC). To enhance exploration, both extrinsic reward r_t^i and intrinsic reward $r_{\text{int},t}^i$ are employed. The intrinsic reward, based on

random network distillation (RND), is computed as the L2 loss between a randomly initialized target network $\hat{f}^i_{\bar{\eta}}$ and a prediction network f^i_η, parameterized by η and $\bar{\eta}$, respectively, and is expressed as:

$$r^i_{\text{int},t} := \left\| f^i_\eta(s_{t+1}) - \hat{f}^i_{\bar{\eta}}(s_{t+1}) \right\|_2^2, \tag{B.2}$$

where i is the task index, and f_η is updated to minimize this loss. A dropout layer is applied to f_η to prevent over-sensitivity to state s. The RL loss functions of SAC for training the skill-improvement policy $\pi_{\text{imp},\psi}$ and the state-action value function $Q_{\text{imp},\psi}$ using the intrinsic reward $r_{\text{int},t}$ are defined as follows:

$$\begin{aligned}
\mathcal{L}^{\text{critic}}_{\text{imp}}(\psi) := \sum_i \mathbb{E}_{\substack{(s_t,a_t,r^i_t,s_{t+1})\sim\mathcal{B}^i_{\text{imp}}\cup\mathcal{B}^i_{\text{on}} \\ a_{t+1}\sim\pi_{\text{imp},\psi}(\cdot|s_t,i)}} \Bigg[\frac{1}{2} \Bigg(Q_{\text{imp},\psi}(s_t,a_t,i) - \Big(\delta_{\text{ext}} r^i_t + \delta_{\text{int}} r^i_{\text{int,t}} + \gamma_{\text{imp}} \big(Q_{\text{imp},\psi}(s_{t+1},a_{t+1},i) \\
+ \lambda^{\text{ent}}_{\text{imp}} \log \pi_{\text{imp},\psi}(a_{t+1}|s_{t+1},i) \big) \Big) \Bigg)^2 \Bigg] \\
\mathcal{L}^{\text{actor}}_{\text{imp}}(\psi) := \sum_i \mathbb{E}_{\substack{s_t\sim\mathcal{B}^i_{\text{imp}}\cup\mathcal{B}^i_{\text{on}} \\ a_t\sim\pi_{\text{imp},\psi}(\cdot|s_t,i)}} \Big[\lambda^{\text{ent}}_{\text{imp}} \log \pi_{\text{imp},\psi}(a_t|s_t,i) - Q_{\text{imp},\psi}(s_t,a_t,i) \Big] - \lambda^{\text{kld}}_{\text{imp}} \sum_i \mathbb{E}_{(s_t,a_t)\sim\mathcal{B}^i_{\text{on}}} \Big[\log \pi_{\text{imp},\psi}(a_t|s_t,i) \Big].
\end{aligned} \tag{B.3}$$

Here, δ_{ext} and δ_{int} are extrinsic and intrinsic reward ratios, γ_{imp} is the discount factor, $\lambda^{\text{ent}}_{\text{imp}}$ is the exploration entropy coefficient adjusted automatically by SAC, and $\lambda^{\text{kld}}_{\text{imp}}$ is the KLD coefficient. Also, note that Eq. (B.3) provides a parameterized and detailed reformulation of Eq. (3) from Section 4.2, explicitly incorporating parameterization and loss scaling details.

To mutually update skill selection based on the refined skills, the updated and fixed low-level skill policy $\bar{\pi}_{l,\phi}$ and skill prior $\bar{q}_\phi$ are utilized to train the high-level policy following the SiMPL framework introduced in Section 3. The objective is to select skill representations z that maximize task returns while ensuring the high-level policy remains close to the skill prior for stable and efficient learning. The high-level policy $\pi_{h,\theta}$ and value function $Q_{h,\theta}$ are parameterized by θ and trained using the soft actor-critic (SAC) framework, with the RL loss functions defined as:

$$\begin{aligned}
\mathcal{L}^{\text{critic}}_h(\theta) := \mathbb{E}_{\substack{(s_t,z_t,r^h_t,s_{t+H_s-1})\sim\mathcal{B}^{\mathcal{T}}_h, e^{\mathcal{T}}\sim q_{e,\theta}(\cdot|c^{\mathcal{T}}) \\ z_{t+1}\sim\pi_{h,\theta}(\cdot|s_{t+H_s-1},e^{\mathcal{T}})}} \Bigg[\frac{1}{2} \Bigg(Q_{h,\theta}(s_t,z_t,e^{\mathcal{T}}) - \Big(r^h_t + \gamma_h \big(Q_{h,\theta}(s_{t+H_s-1},z_{t+1},e^{\mathcal{T}}) \\
- \lambda^{\text{kld}}_h \mathcal{D}_{\text{KL}} \big(\pi_{h,\theta}(\cdot|s_{t+H_s-1},e^{\mathcal{T}}) \,\big\|\, \bar{p}_\phi(\cdot|s_{t+H_s-1}) \big) \big) \Big) \Bigg)^2 \Bigg] \\
\mathcal{L}^{\text{actor}}_h(\theta) := \mathbb{E}_{\substack{s_t\sim\mathcal{B}^{\mathcal{T}}_h, e^{\mathcal{T}}\sim q_{e,\theta}(\cdot|c^{\mathcal{T}}) \\ z_t\sim\pi_{h,\theta}(\cdot|s_t,e^{\mathcal{T}})}} \Big[\lambda^{\text{kld}}_h \mathcal{D}_{\text{KL}} \Big(\pi_{h,\theta}(\cdot|s_t,e^{\mathcal{T}}) \,\Big\|\, \bar{p}_\phi(\cdot|s_t) \Big) - Q_{h,\theta}(s_t,z_t,e^{\mathcal{T}}) \Big],
\end{aligned} \tag{B.4}$$

where $q_{e,\theta}$ is the parameterized task encoder with parameter θ, γ_h is the high-level discount factor, and λ^{kld}_h is the high-level KLD coefficient. The term $r^h_t = \sum_{k=t}^{t+H_s-1} r_k$ represents the cumulative rewards, with states and rewards obtained by executing the low-level skill policy $\bar{\pi}_{l,\phi}$ using $z_t \sim \pi_{h,\theta}(\cdot|s_t)$ over H_s timesteps. The context $c^{\mathcal{T}} = (s_k, z_k, r^h_k, s_{k+H_s-1})_{k=1}^{N_{\text{prior}}}$, where N_{prior} is the number of context transitions, denotes the high-level transition set of task $\mathcal{T}$. This context is used to select the task representation $e^{\mathcal{T}}$ from the task encoder $q_{e,\theta}$. Also, note that Eq. (B.4) is a parameterized modification of Eq. (2) from Section 3.

Self-Improvement Skill Learning

To extract better trajectories and learn skills that effectively solve tasks, the online buffer $\mathcal{B}^i_{\text{on}}$ selectively stores high-return trajectories collected during the meta-training phase through the execution of the low-level policy $\pi_{l,\phi}$ and the skill-improvement policy $\pi_{\text{imp},\psi}$. A trajectory τ^i is added to $\mathcal{B}^i_{\text{on}}$ if its return $G(\tau^i)$ exceeds the minimum return in the buffer, $\min_{\tau'\in\mathcal{B}^i_{\text{on}}} G(\tau')$. To refine skills, maximum return relabeling is applied using the parameterized reward model $\hat{R}_\zeta$ with parameter ζ. The reward model is trained by minimizing the following MSE loss:

$$\mathcal{L}_{\text{reward}}(\zeta) := \mathbb{E}_{(s^i_t,a^i_t,r^i_t)\sim\mathcal{B}^i_{\text{imp}}\cup\mathcal{B}^i_{\text{on}}} \Big[\Big(\hat{R}_\zeta(s^i_t,a^i_t,i) - r^i_t \Big)^2 \Big]. \tag{B.5}$$

This assigns priorities to offline trajectories $\tilde{\tau} \in \mathcal{B}_{\text{off}}$ (Eq. (5)), updated for N_{priority} samples per iteration.

For skill learning, the low-level skill policy $\pi_{l,\phi}$, skill encoder q_ϕ, and skill prior p_ϕ are optimized using the following loss function. This incorporates both high-return trajectories from the online buffer $\mathcal{B}^i_{\text{on}}$ and trajectories from the offline buffer $\mathcal{B}_{\text{off}}$, weighted by their importance:

$$\begin{aligned}\mathcal{L}_{\text{skill}}(\phi) := (1-\beta)\mathbb{E}_{\substack{(s_{t:t+H_s},a_{t:t+H_s})\sim P_{\mathcal{B}_{\text{off}}} \\ z\sim q_\phi(\cdot|s_{t:t+H_s},a_{t:t+H_s})}}\Big[\mathcal{L}(\pi_{l,\phi},q_\phi,p_\phi,z)\Big] \\ + \frac{\beta}{N_{\mathcal{T},\text{train}}}\sum_i \mathbb{E}_{\substack{(s_{t:t+H_s},a_{t:t+H_s})\sim \mathcal{B}^i_{\text{on}} \\ z\sim q_\phi(\cdot|s_{t:t+H_s},a_{t:t+H_s})}}\Big[\mathcal{L}(\pi_{l,\phi},q_\phi,p_\phi,z)\Big],\end{aligned} \tag{B.6}$$

where β is the mixing coefficient defined in Eq. (7), and $\mathcal{L}(\pi_{l,\phi}, q_\phi, p_\phi, z)$ is the skill learning objective defined in Eq. (B.1) for optimizing $\pi_{l,\phi}$, q_ϕ, and p_ϕ. During training, we update the low-level policy $\bar{\pi}_{l,\phi}$, skill encoder $\bar{q}_\phi$, and skill prior $\bar{p}_\phi$ used for the skill-based meta-RL every K_{iter} iterations. Specifically, the updates are performed as follows: $\bar{\pi}_{l,\phi} \leftarrow \pi_{l,\phi}$, $\bar{q}_\phi \leftarrow q_\phi$, and $\bar{p}_\phi \leftarrow p_\phi$.

B.3 Meta-Test Phase

After completing the meta-train phase of SISL, the meta-test phase is performed on the test task set $\mathcal{M}_{\text{test}}$. In this phase, previously learned components, including the task encoder $q_{e,\theta}$, low-level skill policy $\bar{\pi}_{l,\phi}$, and skill prior $\bar{p}_\phi$, are kept fixed and are no longer updated. Only the high-level policy $\pi_{h,\theta}$ and high-level value function $Q_{h,\theta}$ are trained for each test task using the soft actor-critic (SAC) framework.

During meta-testing, for each test task $\mathcal{T}$, the task representation $e^{\mathcal{T}}$ is inferred from the fixed task encoder $q_{e,\theta}$. The SAC algorithm is then applied to optimize the high-level policy and value function for the specific test task, following the same loss functions as defined in Eq. (B.4) from the meta-training phase. This approach ensures efficient adaptation to unseen tasks by leveraging the fixed, pre-trained low-level skills and task representations.

Algorithm 1: SISL: Meta-Train Phase

Require: Training tasks $\mathcal{M}_{\text{train}}$, offline dataset $\mathcal{B}_{\text{off}}$, low-level policy $\pi_{l,\phi}$, skill encoder q_ϕ, and skill prior p_ϕ.

Initialize: High-level policy $\pi_{h,\theta}$, skill-improvement policy $\pi_{\text{imp},\psi}$, task encoder $q_{e,\theta}$, reward model $\hat{R}_\zeta$, and value functions $Q_{h,\theta}$, $Q_{\text{imp},\psi}$.

Fix $\bar{\pi}_{l,\phi} \leftarrow \pi_{l,\phi}$, $\bar{q}_\phi \leftarrow q_\phi$, and $\bar{p}_\phi \leftarrow p_\phi$.
for iteration $k = 1, 2, \cdots$ **do**
  for task $i = 1$ **to** $N_{\mathcal{T},\text{train}}$ **do**
    Collect high-level trajectories τ_h^i and low-level trajectories τ_l^i using $\pi_{h,\theta}$ with $\bar{\pi}_{l,\phi}$, $q_{e,\theta}$.
    Collect skill-improvement trajectories τ_{imp}^i using $\pi_{\text{imp},\psi}$.
    Filter high-return trajectories τ_{high}^i from τ_l^i and τ_{imp}^i s.t. $G > \min_{\tau' \in \mathcal{B}_{\text{on}}^i} G(\tau')$.
    Store τ_h^i, τ_{imp}^i, and τ_{high}^i into $\mathcal{B}_h^i$, $\mathcal{B}_{\text{imp}}^i$, and $\mathcal{B}_{\text{on}}^i$.
  Compute prioritization factors: $P_{\mathcal{B}_{\text{off}}}$ and β.
  for gradient step **do**
    (Decoupled Policy Learning)
    Update $\pi_{\text{imp},\psi}$, $Q_{\text{imp},\psi}$ using Eq. (B.3) with $\psi \leftarrow \psi - \lambda_{\text{imp}}^{\text{lr}} \cdot \nabla_\psi(\mathcal{L}_{\text{imp}}^{\text{critic}}(\psi) + \mathcal{L}_{\text{imp}}^{\text{actor}}(\psi))$.
    Update $\pi_{h,\theta}$, $Q_{h,\theta}$, $q_{e,\theta}$ using Eq. (B.4) with $\theta \leftarrow \theta - \lambda_h^{\text{lr}} \cdot \nabla_\theta(\mathcal{L}_h^{\text{critic}}(\theta) + \mathcal{L}_h^{\text{actor}}(\theta))$.
    (Self-Improvement Skill Learning)
    Update reward model $\hat{R}_\zeta$ using Eq. (B.5) with $\zeta \leftarrow \zeta - \lambda_{\text{reward}}^{\text{lr}} \cdot \nabla_\zeta \mathcal{L}_{\text{reward}}(\zeta)$.
    Update $\pi_{l,\phi}$, q_ϕ, p_ϕ using Eq. (B.6) with $\phi \leftarrow \phi - \lambda_l^{\text{lr}} \cdot \nabla_\phi \mathcal{L}_{\text{skill}}(\phi)$.
  if $k \bmod K_{\text{iter}} = 0$ **then**
    Update $\bar{\pi}_{l,\phi} \leftarrow \pi_{l,\phi}$, $\bar{q}_\phi \leftarrow q_\phi$, and $\bar{p}_\phi \leftarrow p_\phi$.
    Reinitialize $\pi_{h,\theta}$.

Algorithm 2: SISL: Meta-test phase

Require: Target task $\mathcal{T}$, high-level policy $\pi_{h,\theta}$, value function $Q_{h,\theta}$, task encoder $q_{e,\theta}$, and low-level policy $\pi_{l,\phi}$.

Collect context $c^{\mathcal{T}}$ using $\pi_{h,\theta}$ with $\pi_{l,\phi}$, $e \sim \mathcal{N}(0, \mathrm{I})$.
Compute task representation $e^{\mathcal{T}} \sim q_{e,\theta}(\cdot|c^{\mathcal{T}})$.
for iteration $k = 1, 2, \ldots$ **do**
  Collect high-level trajectory $\tau_h^{\mathcal{T}}$ using $\pi_{h,\theta}$ with $\pi_{l,\phi}$, $e^{\mathcal{T}}$.
  Store $\tau_h^{\mathcal{T}}$ into $\mathcal{B}_h^{\mathcal{T}}$.
  for gradient step **do**
    Update $\pi_{h,\theta}$, $Q_{h,\theta}$ using Eq. (B.4) with $\theta \leftarrow \theta - \lambda_h^{\text{lr}} \cdot \nabla_\theta(\mathcal{L}_h^{\text{critic}}(\theta) + \mathcal{L}_h^{\text{actor}}(\theta))$

C Detailed Experimental Setup

In this section, we provide a detailed description of our experimental setup. The implementation is built on PyTorch with CUDA 11.7, running on an AMD EPYC 7313 CPU with an NVIDIA GeForce RTX 3090 GPU. SISL is implemented based on the official open-source code of SiMPL, available at https://github.com/namsan96/SiMPL. For the environment implementations, we used SiMPL's code for the Kitchen and Maze2D environments, SkiLD's open-source code for the Office environment at https://github.com/clvrai/skild, and D4RL's open-source code for AntMaze at https://github.com/Farama-Foundation/D4RL/tree/master.

The hyperparameters for low-level policy training were referenced from SPiRL (Pertsch et al., 2021). Additional details about the baseline algorithms are provided in Section C.1, while Section C.2 elaborates on the environments used for evaluation. Section C.3 explains the construction of offline datasets for varying noise levels, and Section C.4 details the network architectures and hyperparameter configurations for policies, value functions, and other models.

C.1 Other Baselines

Here are the detailed descriptions and implementation details of the algorithms used for performance comparison:

SAC
SAC (Haarnoja et al., 2018) is a reinforcement learning algorithm that incorporates entropy to improve exploration. Instead of a standard value function, SAC uses a soft value function that combines entropy, with the entropy coefficient adjusted automatically to maintain the target entropy. To enhance value function estimation, SAC employs double Q learning, using two independent value functions. SAC learns tasks from scratch without utilizing meta-train tasks or offline datasets. For the Kitchen and Office environments, the discount factor γ is set to 0.95, while $\gamma = 0.99$ is used for Maze2D and AntMaze environments. We utilize the open-source code of SAC at https://github.com/denisyarats/pytorch_sac.

SAC+RND
SAC+RND combines SAC with random network distillation (RND) (Burda et al., 2018), an intrinsic motivation technique, to enhance exploration. Like SAC, it learns tasks from scratch without meta-train tasks or offline datasets. RL hyperparameters are shared with SAC, and RND-specific hyperparameters are set to match those in SISL. Additionally, for fair comparison, the ratio of extrinsic to intrinsic rewards is aligned with SISL. We utilize the open-source code of RND at https://github.com/openai/random-network-distillation.

PEARL
PEARL (Rakelly et al., 2019) is a context-based meta-RL algorithm that leverages a task encoder q_e to derive task representations, which are then used to train a meta-policy. PEARL adapts its learned policy quickly to unseen tasks without utilizing skills or offline datasets. Unlike the original PEARL, which does not fine-tune during the meta-test phase, we modified it to include fine-tuning on target tasks for a fair comparison. We utilize the open-source code of PEARL at https://github.com/katerakelly/oyster.

PEARL+RND
PEARL+RND extends PEARL by incorporating RND to enhance exploration. Like SAC+RND, the ratio of extrinsic to intrinsic rewards is set to match SISL for fair comparison.

SPiRL
SPiRL (Pertsch et al., 2021) is a skill-based RL algorithm that first learns a fixed low-level policy from an offline dataset and then trains a high-level policy for specific tasks. SPiRL's loss function is detailed in Section 3, and for fair comparison, loss scaling is aligned with SISL. We utilize the open-source code of SPiRL at https://github.com/clvrai/spirl.

SiMPL
SiMPL (Nam et al., 2022) is a skill-based meta-RL algorithm that uses both offline datasets and meta-train tasks. While it shares SISL's approach of extracting reusable skills and performing meta-train and meta-test phases, SiMPL fixes the skill model without further updates during meta-training. SiMPL's loss function is also detailed in Section 3, and SiMPL's implementation uses the same hyperparameters as SISL to ensure a fair comparison. We utilize the open-source code of SiMPL at https://github.com/namsan96/SiMPL.

C.2 Environmental Details

Kitchen

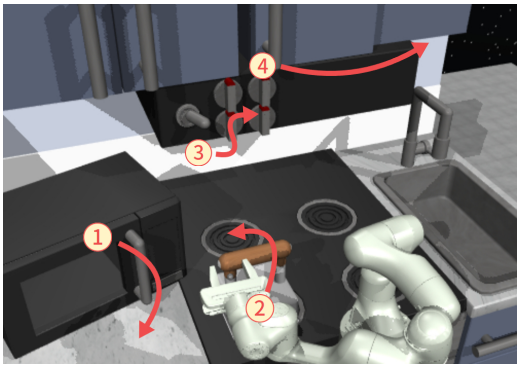

Figure C.1: Kitchen: An example of task (microwave→kettle→bottom burner→slide cabinet)

The Franka Kitchen environment is a robotic manipulation setup based on the 7-DoF Franka robot. It is introduced by Gupta et al. (2020) and later adapted by Nam et al. (2022) to exclude task information from the observation space, making it more suitable for meta-learning. The environment features seven manipulatable objects: bottom burner, top burner, light switch, slide cabinet, hinge cabinet, microwave, and kettle.

Each subtask involves manipulating one object to its target state, while a full task requires sequentially completing four subtasks. The agent earns a reward of 1 for each completed subtask, with a maximum score of 4 achievable within a 280-timestep horizon. For instance, an example task, illustrated in Fig. C.1, requires the agent to complete the sequence: microwave → kettle → bottom burner → slide cabinet. The observation space is a 60-dimensional continuous vector representing object positions and robot state information, while the action space is a 9-dimensional continuous vector. Based on the task setup from Nam et al. (2022), we expanded the meta-train task set by adding two additional tasks, resulting in a total of 25 meta-train tasks and 10 meta-test tasks. Detailed task configurations are provided in Table C.1.

Table C.1: List of meta-train tasks and meta-test tasks in Kitchen environment

Meta-train task					Meta-test task				
#	Subtask1	Subtask2	Subtask3	Subtask4	#	Subtask1	Subtask2	Subtask3	Subtask4
1	microwave	kettle	bottom burner	slide cabinet	1	microwave	bottom burner	light switch	top burner
2	microwave	bottom burner	top burner	slide cabinet	2	microwave	bottom burner	top burner	light switch
3	microwave	top burner	light switch	hinge cabinet	3	kettle	bottom burner	light switch	slide cabinet
4	kettle	bottom burner	light switch	hinge cabinet	4	microwave	kettle	top burner	hinge cabinet
5	microwave	bottom burner	hinge cabinet	top burner	5	kettle	bottom burner	slide cabinet	top burner
6	kettle	top burner	light switch	slide cabinet	6	kettle	light switch	slide cabinet	hinge cabinet
7	microwave	kettle	slide cabinet	bottom burner	7	kettle	bottom burner	top burner	slide cabinet
8	kettle	light switch	slide cabinet	bottom burner	8	microwave	bottom burner	slide cabinet	hinge cabinet
9	microwave	kettle	bottom burner	top burner	9	bottom burner	top burner	slide cabinet	hinge cabinet
10	microwave	kettle	slide cabinet	hinge cabinet	10	microwave	kettle	bottom burner	hinge cabinet
11	microwave	bottom burner	slide cabinet	top burner					
12	kettle	bottom burner	light switch	top burner					
13	microwave	kettle	top burner	light switch					
14	microwave	kettle	light switch	hinge cabinet					
15	microwave	bottom burner	light switch	slide cabinet					
16	kettle	bottom burner	top burner	light switch					
17	microwave	light switch	slide cabinet	hinge cabinet					
18	microwave	bottom burner	top burner	hinge cabinet					
19	kettle	bottom burner	slide cabinet	hinge cabinet					
20	bottom burner	top burner	slide cabinet	light switch					
21	microwave	kettle	light switch	slide cabinet					
22	kettle	bottom burner	top burner	hinge cabinet					
23	bottom burner	top burner	light switch	slide cabinet					
24	top burner	hinge cabinet	microwave	slide cabinet					
25	bottom burner	hinge cabinet	light switch	kettle					

Office

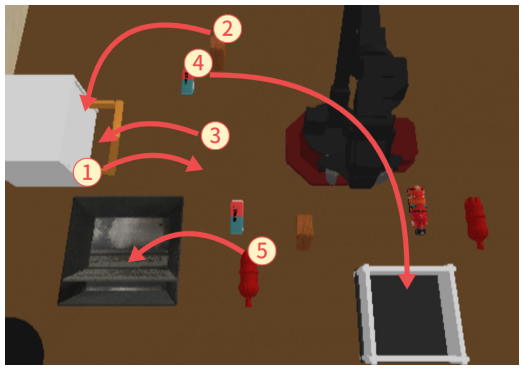

Figure C.2: Office: An example of task ((shed2, drawer)→(eraser1, container)→(pepsi2, tray))

The Office environment is a robotic manipulation setup featuring a 5-DoF robotic arm. Originally proposed by Pertsch et al. (2022), it has been modified to accommodate meta-learning tasks. The environment simulates an office cleaning scenario with seven objects (eraser1, shed1, pepsi1, gatorade, eraser2, shed2, pepsi2) and three organizers (tray, container, drawer).

The goal is to move objects to their designated organizers, with each object-to-organizer transfer constituting a subtask. A full task involves completing three sequential subtasks, where a subtask is defined as an (object, organizer) pair. For tasks involving a tray or container, the agent earns a reward of 1 for both picking and placing the object. For tasks involving the drawer, the agent receives 1 reward point for each of the following actions: opening the drawer, picking, placing, and closing the drawer. This scoring setup allows for a maximum score of 8 within a 300-timestep horizon.

An example task, depicted in Fig. C.2, requires the agent to sequentially complete: (shed2 → drawer), (eraser1 → container), and (pepsi2 → tray). The observation space is a 76-dimensional continuous vector, including object positions and robot state information, while the action space is an 8-dimensional continuous vector. The meta-train and meta-test sets include 25 and 10 tasks, respectively, similar to the configuration in the Kitchen environment. A detailed task list is provided in Table C.2.

Table C.2: List of meta-train tasks and meta-test tasks in Office environment

Meta-train task				Meta-test task			
#	Subtask1	Subtask2	Subtask3	#	Subtask1	Subtask2	Subtask3
1	(shed2, drawer)	(eraser1, container)	(pepsi2, tray)	1	(gatorade, drawer)	(eraser1, tray)	(pepsi2, container)
2	(shed2, container)	(eraser1, drawer)	(pepsi1, tray)	2	(eraser1, drawer)	(eraser2, container)	(pepsi1, tray)
3	(eraser1, tray)	(shed2, drawer)	(gatorade, container)	3	(eraser2, drawer)	(pepsi1, tray)	(gatorade, container)
4	(pepsi1, tray)	(eraser1, container)	(eraser2, drawer)	4	(shed2, drawer)	(pepsi2, tray)	(pepsi1, container)
5	(shed1, tray)	(shed2, drawer)	(pepsi2, container)	5	(shed2, container)	(gatorade, tray)	(eraser1, drawer)
6	(pepsi1, container)	(shed1, tray)	(eraser2, drawer)	6	(gatorade, container)	(eraser2, drawer)	(pepsi2, tray)
7	(gatorade, tray)	(eraser2, container)	(eraser1, drawer)	7	(gatorade, tray)	(shed1, container)	(eraser1, drawer)
8	(pepsi2, container)	(shed2, drawer)	(eraser1, tray)	8	(pepsi2, drawer)	(shed1, tray)	(pepsi1, container)
9	(shed2, drawer)	(gatorade, container)	(pepsi2, tray)	9	(pepsi1, tray)	(pepsi2, container)	(shed2, drawer)
10	(eraser1, container)	(pepsi2, drawer)	(shed1, tray)	10	(gatorade, drawer)	(pepsi1, container)	(eraser2, tray)
11	(eraser2, drawer)	(shed2, tray)	(pepsi2, container)				
12	(pepsi2, container)	(shed2, drawer)	(shed1, tray)				
13	(shed2, tray)	(pepsi1, container)	(eraser1, drawer)				
14	(gatorade, tray)	(eraser1, drawer)	(pepsi1, container)				
15	(eraser1, tray)	(shed1, drawer)	(gatorade, container)				
16	(eraser2, drawer)	(gatorade, container)	(shed2, tray)				
17	(shed2, tray)	(pepsi2, drawer)	(shed1, container)				
18	(pepsi1, container)	(pepsi2, tray)	(eraser1, drawer)				
19	(shed2, tray)	(gatorade, drawer)	(shed1, container)				
20	(gatorade, tray)	(pepsi1, container)	(pepsi2, drawer)				
21	(eraser1, tray)	(shed2, drawer)	(pepsi2, container)				
22	(eraser1, tray)	(gatorade, drawer)	(shed2, container)				
23	(pepsi1, container)	(shed2, drawer)	(eraser2, tray)				
24	(gatorade, drawer)	(shed1, tray)	(pepsi2, container)				
25	(eraser2, container)	(pepsi1, drawer)	(eraser1, tray)				

Maze2D

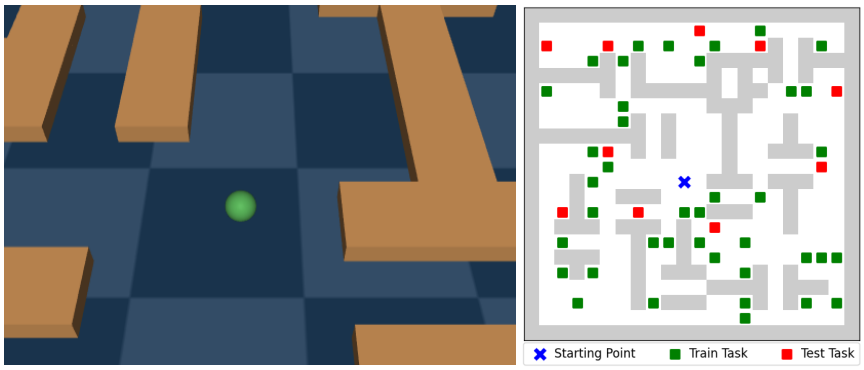

(a) Simulation (b) Training and test tasks

Figure C.3: Maze2D: Visualization of simulation and meta-train/test tasks in Maze2D

The Maze2D environment is a navigation setup where a 2-DoF ball agent moves toward a goal point. Initially introduced by Fu et al. (2020b) and later adapted by Nam et al. (2022) for meta-learning tasks, the environment is defined on a 20x20 grid. The agent receives a reward of 1 upon reaching the goal point within a horizon of 2000 timesteps.

Fig. C.3 (a) provides a visualization of the Maze2D environment, while Fig. C.3 (b) illustrates the meta-train and meta-test tasks. In Fig. C.3 (b), green squares indicate the goal points for 40 meta-train tasks, and red squares represent the goal points for 10 meta-test tasks. All tasks share the same starting point at (10, 10), marked by a blue cross. The observation space is a 4-dimensional continuous vector containing the ball's position and velocity, while the action space is a 2-dimensional continuous vector.

AntMaze

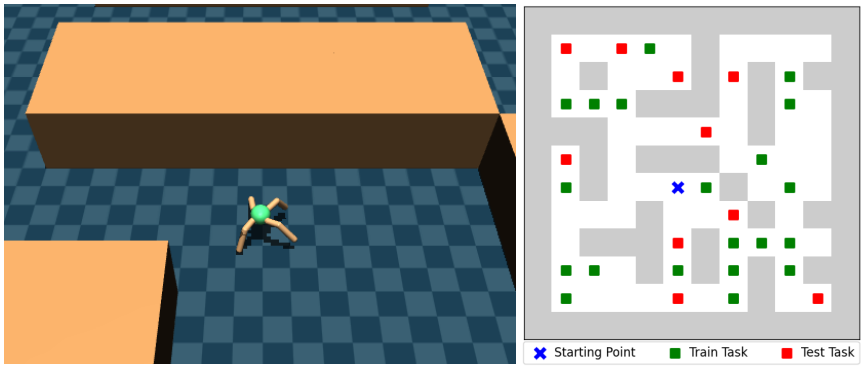

(a) Simulation (b) Training and test tasks

Figure C.4: AntMaze: Visualization of simulation and meta-train/test tasks in AntMaze

The AntMaze environment combines navigation and locomotion, replacing the 2-DoF ball from the Maze2D environment with a more complex 8-DoF quadruped Ant robot. Initially proposed by Fu et al. (2020b) and later adapted for meta-learning setups, the environment is defined on a 10x10 grid. The agent receives a reward of 1 upon reaching the goal point within a horizon of 1000 timesteps.

Fig. C.4 (a) shows a simulation image of the AntMaze environment, and Fig. C.4 (b) depicts the meta-train and meta-test tasks. In Fig. C.4 (b), green squares mark the goal points for 20 meta-train tasks, while red squares denote the goal points for 10 meta-test tasks. All tasks share a common starting point at (5, 5), indicated by a blue cross. The observation space is a 29-dimensional continuous vector that includes the Ant's state and its (x, y) coordinates, while the action space is an 8-dimensional continuous vector.

C.3 Construction of Offline Dataset

In this section, we detail the offline datasets used in our experiments. For the Office, Maze2D, and AntMaze environments, we employ rule-based oracle controllers provided by each environment. The Office oracle controller is available at https://github.com/clvrai/skild, while the Maze2D and AntMaze oracle controllers can be found in https://github.com/Farama-Foundation/D4RL/tree/master. For the Kitchen environment, which only provides human demonstrations, we train a policy using behavior cloning to serve as the oracle controller.

For the Kitchen environment, 1M transitions are collected using 25 tasks that are not part of the training or test task sets $\mathcal{M}_{\text{train}} \cup \mathcal{M}_{\text{test}}$. Similarly, the Office environment collects 1M transitions using 80 tasks. The Maze2D and AntMaze environments follow the same approach, collecting 0.5M transitions using 40 and 50 tasks respectively, with randomly sampled initial and goal points. Unlike SiMPL, which randomly samples initial and goal points for each trajectory in the Maze2D environment, we limit our data collection to 40 distinct tasks, resulting in trajectories that do not fully cover the map. To introduce noise in the demonstrations, Gaussian noise with various standard deviations σ is added to the oracle controller's actions. For the Kitchen and Office environments, noise levels of $\sigma = 0.1, 0.2,$ and 0.3 are used, while for Maze2D and AntMaze, $\sigma = 0.5, 1.0,$ and 1.5 are applied.

C.4 HYPERPARAMETER SETUP

In this section, we outline the hyperparameter setup for the proposed SISL framework. For high-level policy training, we adopt the hyperparameters from SiMPL for the Kitchen and Maze2D environments. For the Office and AntMaze environments, we conduct hyperparameter sweeps using the Kitchen and Maze2D configurations as baselines.

To ensure a fair comparison, we inherit from SiMPL all hyperparameters that are shared with SISL, given its multiple loss functions, and we perform parameter sweeps only over SISL specific components, namely self-improving skill refinement and skill prioritization via maximum return relabeling. We explore prioritization temperature values $T \in [0.1, 0.5, 1.0, 2.0]$ and KLD coefficients $\lambda^{\text{kld}}_{\text{imp}} \in [0, 0.001, 0.002, 0.005]$ for skill exploration, selecting the best-performing configurations as defaults. Additionally, the ratio of intrinsic to extrinsic rewards is fixed at levels that show optimal performance in single-task SAC experiments.

For implementing the skill models (π_l, q, p), we follow SPiRL by utilizing LSTM (Graves & Graves, 2012) for the skill encoder and MLP structures for the low-level skill policy and skill prior. For implementing the high-level models (π_h, Q_h, q_e), we follow SiMPL by utilizing Set Transformer (Lee et al., 2019) for the task encoder and MLP structures for the high-level policy and value function. Additionally, for implementing the SISL, we utilize MLP structures for π_{imp}, Q_{imp}, and $\hat{R}$. The detailed hidden network sizes are presented in Table C.3 and Table C.4. Table C.3 presents the network architectures (the number of nodes in fully connected layers) and the hyperparameters shared across all environments, while Table C.4 details the environment-specific hyperparameter setups.

Table C.3: Network Architecture and Shared Hyperparameters

	Group	Name	Environments			
			Kitchen	Office	Maze2D	AntMaze
Shared Hyperparameters	High-level	Discount Factor γ_h	0.99			
		Learning rate λ^{lr}_h	0.0003			
		Network size π_h, Q_h	[128]×6		[256]×4	[128]×6
	Low-level	Buffer size $\mathcal{B}^i_{\text{on}}$	10K			
		KLD coefficient λ^{kld}_l	0.0005			
		Skill length H_s	10			
		Skill dimension $\dim(z)$	10			
		# of priority update trajectory N_{priority}	200			
		Learning rate $\lambda^{\text{lr}}_{\text{skill}}$	0.001			
		Learning rate $\lambda^{\text{lr}}_{\text{reward}}$	0.0003			
		Network size $\hat{R}$	[128]×3			
		Network size π_l	[128]×6			
		Network size p	[128]×7			
		Network size q	LSTM[128]			
	Skill-Improvement	RND state dropout ratio	0.7			
		RND output dimension	10			
		Learning rate $\lambda^{\text{lr}}_{\text{imp}}$	0.0003			
		Network size $\pi_{\text{imp}}, Q_{\text{imp}}$	[256]×4			
		Network size $f, \hat{f}$	[128]×4			

Table C.4: Environmental Hyperparameters

	Group	Name	Environments			
			Kitchen	Office	Maze2D	AntMaze
Environmental Hyperparameters	High-level	Buffer size $\mathcal{B}^i_h$	3000	3000	20000	20000
		KLD coefficient λ^{kld}_h	0.03	0.03	0.001	0.0003
		Task latent dimension $\dim(e)$	5	5	6	6
		Batch size (RL, per task)	256	256	1024	512
		Batch size (context, per task)	1024	1024	8192	4096
	Low-level	Skill refinement K_{iter}	2000	2000	1000	2000
		Prioritization temperature T	1.0	1.0	0.5	0.5
	Skill-Improvement	Buffer size $\mathcal{B}^i_{\text{imp}}$	100K	200K	100K	300K
		Discount factor γ_{imp}	0.95	0.95	0.99	0.99
		RND extrinsic ratio δ_{ext}	5	2	10	10
		RND intrinsic ratio δ_{int}	0.1	0.1	0.01	0.01
		Entropy coefficient $\lambda^{\text{ent}}_{\text{imp}}$	0.2	0.2	0.1	0.1
		KLD coefficient $\lambda^{\text{kld}}_{\text{imp}}$	0.005 (Expert) 0.005 ($\sigma = 0.1$) 0.002 ($\sigma = 0.2$) 0.001 ($\sigma = 0.3$)		0.001	0.001	0.001

D Additional Comparison Results

In this section, we provide additional comparison results against baseline algorithms. Following Fig. 6, additional performance comparisons across all environments and noise levels are presented in Section D.1, limited offline dataset size in Section D.2, random noise injection in Section D.3, and diverse sub-optimal offline datasets in Section D.4.

D.1 Performance Comparison

Fig. D.1 presents the learning curves of average returns for the algorithms on test tasks, corresponding to the experiments summarized in Table 1. Rows represent evaluation environments, and columns denote noise levels. SISL consistently demonstrated superior robustness, outperforming all baselines across various environments and noise levels. At higher noise levels such as Noise($\sigma = 0.2$), Noise($\sigma = 0.3$) for Kitchen and Office, and Noise($\sigma = 1.0$), Noise($\sigma = 1.5$) for Maze2D and AntMaze, significant performance improvements highlight the effectiveness of skill refinement in addressing noisy demonstrations. Even with high-quality offline datasets like Expert and Noise($\sigma = 0.1$) for Kitchen and Office, and Noise($\sigma = 0.5$) for Maze2D and AntMaze, SISL further improved performance by learning task-relevant skills. These learning curves align with the trends observed in the main experiments, confirming that skill refinement enhances performance across various dataset qualities and effectively adapts to the task distribution.

Interestingly, SPiRL and SiMPL sometimes perform better with mild Gaussian noise than with expert data, especially in Maze2D and AntMaze. Our analysis suggests that mild noise increases the diversity of behaviors in the dataset without significantly reducing success rates, allowing agents to reach goals via more diverse paths. This expands state-action coverage (by about 7.3% in Maze2D and 5.2% in AntMaze), helping skill-based methods learn more flexible and reusable skills. However, as the noise level increases further, a significant portion of trajectories fail to reach the goal, leading to low quality skill learning and degraded downstream performance.

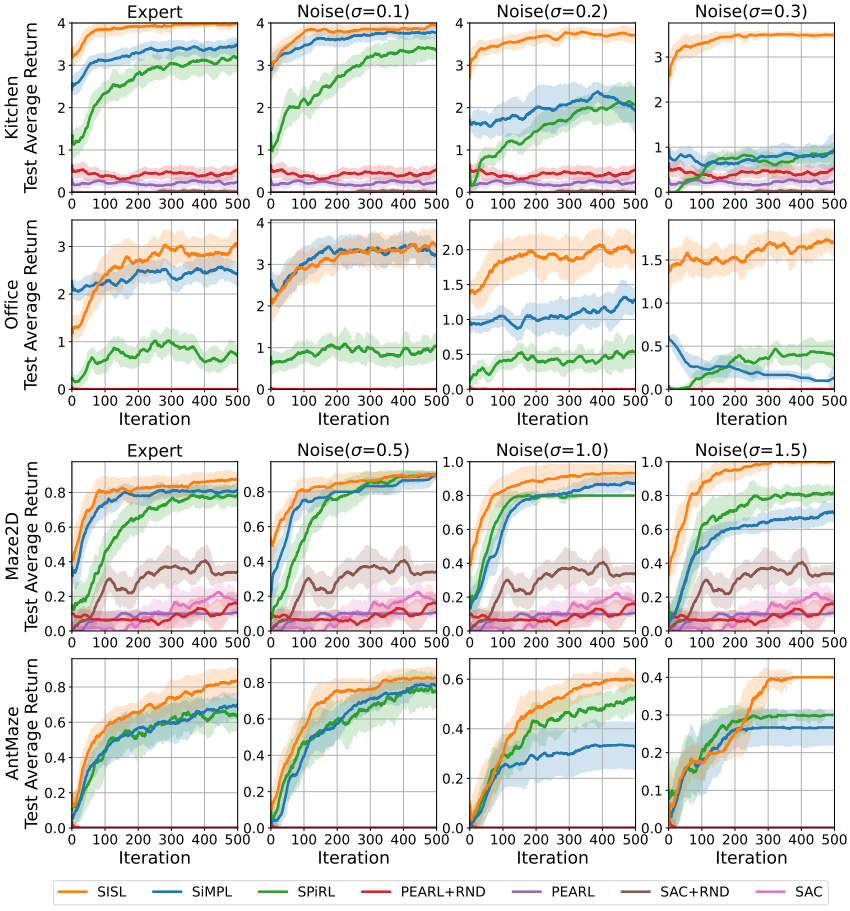

Figure D.1: Learning curves across considered environments and noise levels

D.2 Limited Offline Dataset Size

To further investigate the robustness of SISL, we conducted additional experiments to assess the impact of dataset size on skill learning and downstream performance. While SISL primarily addresses the challenge of refining corrupted skills from noisy demonstrations through online interaction, the size of the offline dataset remain important factors, especially in practical scenarios. To assess the impact of dataset size, we conducted additional experiments on the Kitchen environment using the same expert dataset but reduced to 50% (0.5M), 25% (0.25M), and 10% (0.1M) of its original dataset size (1M). As shown in Table D.1, SISL consistently outperforms baselines even under limited expert data, and its performance degrades more gracefully compared to baselines. These results confirm SISL's ability to refine skills even from limited data, which is particularly valuable in real-world scenarios where collecting high-quality demonstrations is costly or infeasible.

Table D.1: Final performance on the Kitchen environment with varying sizes of expert datasets.

Dataset Size	SPiRL	SiMPL	SISL
Expert(100%)	3.11±0.33	3.40±0.18	**3.97**±0.09
Expert(50%)	3.11±0.30	3.29±0.18	**3.65**±0.06
Expert(25%)	2.91±0.29	2.99±0.13	**3.60**±0.14
Expert(10%)	2.37±0.28	2.56±0.09	**3.28**±0.15

D.3 Random Noise Injection

While Gaussian noise is a widely used approach for degrading demonstration quality in offline RL studies, it does not fully capture the diverse and unstructured nature of real-world noise such as sensor failures, occlusions, or actuator malfunctions. In our main experiments, we adopted multi-level Gaussian noise for two reasons: (1) it is a standard and accepted method for systematically degrading demonstration quality, and (2) it enables controlled analysis of robustness under varying degrees of skill degradation. Notably, in domains such as Kitchen and Office, sufficiently high levels of Gaussian noise render learned skills nearly unusable, effectively mimicking real-world failure scenarios in precision control tasks and providing a highly challenging regime for evaluating robustness.

To further assess the generality of our robustness claims and address concerns about the limitations of Gaussian noise, we conducted an additional experiment using random action injection in the Kitchen environment. This approach better simulates real-world anomalies such as actuator faults or sensor failures. Specifically, at each timestep, the oracle action was replaced with a randomly sampled action with a probability of 25%, 50%, or 100% (resulting in a uniformly random dataset at the highest level). This method introduces severe, unstructured corruption into the offline dataset, representing worst-case real-world failures beyond the smooth degradations induced by Gaussian noise. As shown in Table D.2, SISL consistently outperformed baseline methods, confirming its robustness even under extreme, non-gaussian corruption. These results demonstrate SISL's ability to refine useful behaviors and maintain strong performance in the presence of severe dataset corruption, further validating the generality of our robustness claims.

Table D.2: Final performance on the Kitchen environment with the random noise injection.

Noise Type	SPiRL	SiMPL	SISL
Expert	3.11±0.33	3.40±0.18	**3.97**±0.09
Injection(25%)	0.80±0.15	0.77±0.12	**3.42**±0.11
Injection(50%)	0.14±0.10	0.04±0.05	**3.26**±0.15
Injection(100%)	0.07±0.08	0.02±0.05	**1.68**±0.18

D.4 DIVERSE SUB-OPTIMAL DATASET

Beyond injecting noise into expert demonstrations, we also considered datasets of diverse quality sub-optimal demonstration. Our decision to focus on noisy expert trajectories stems from the specific challenge we aim to address. Unlike offline-RL, which typically assumes access to reward-labeled trajectories and aims to improve performance from sub-optimal data, our setup considers reward-free offline data where noise degrades originally near-optimal demonstrations. This setting better reflects our goal of studying how exploration can help enhance skill learning when clean supervision is unavailable. To test whether robustness hold across different data qualities, we conducted additional experiments in the Kitchen domain using three dataset types: expert (return $= 4$), medium (return ≈ 2), and random (collected from a uniformly random policy). As summarized in Table D.3, SISL consistently outperforms other methods across all dataset types, further validating its robustness to data sub-optimality.

Table D.3: Final performance on the Kitchen environment with diverse quality of offline datasets.

Dataset	SPiRL	SiMPL	SISL
Expert	$3.11_{\pm 0.33}$	$3.40_{\pm 0.18}$	$\mathbf{3.97}_{\pm 0.09}$
Medium	$2.62_{\pm 0.27}$	$3.17_{\pm 0.26}$	$\mathbf{3.77}_{\pm 0.21}$
Random	$0.07_{\pm 0.08}$	$0.02_{\pm 0.05}$	$\mathbf{1.68}_{\pm 0.18}$

E COMPUTATIONAL COMPLEXITY

Despite SISL's significant performance improvements on noisy demonstrations through self-improving skill refinement, it is important to consider the computational trade-offs. Simultaneously training both low-level and high-level policies in SISL can increase computation time. During meta-train, SISL requires approximately 16% more time per iteration (SiMPL: 15.1s vs SISL: 17.6s in Kitchen). However, as shown in Fig. 6, SiMPL does not improve under high-noise settings even with extended training, whereas SISL continues to improve, justifying this computational overhead. Importantly, considering that the main goal of meta-RL is adaptation to unseen tasks, SISL does not require additional computational cost during the fine-tuning phase and maintains similar computation time as SiMPL in the meta-test phase while still achieving superior performance compared to baseline algorithms.

F Further Analysis Results for the SISL Framework

In this section, we provide a more detailed analysis and visualization results of the skill refinement process in the SISL. The analysis performed includes the evolution of the mixing coefficient β in Section F.1, visualization of the refined skills and the corresponding skill sequence visualization in Section F.2, task representation in Section F.3, and the learning stability of the reward model during the meta-train phase in Section F.4.

F.1 Evolution of The Mixing Coefficient β

Fig. F.1 illustrates the evolution of the mixing coefficient β during the meta-train phase across all environments and noise levels. Initially, low β values reflect reliance on offline datasets for skill learning, particularly in high-return environments like Kitchen and Office, where training starts with β values close to zero. This approach prevents performance degradation by avoiding early dependence on lower-quality online samples, while ensuring gradual and stable changes in the skill distribution. As training progresses, the quality of online samples improves, leading to a gradual increase in β, which facilitates greater utilization of online data for skill refinement. For offline datasets with higher noise levels, β converges to higher values. Consequently, SISL learns increasingly effective skills as training proceeds, achieving superior performance on unseen tasks, underscoring the importance of SISL's ability to dynamically balance the use of offline and online data based on dataset quality.

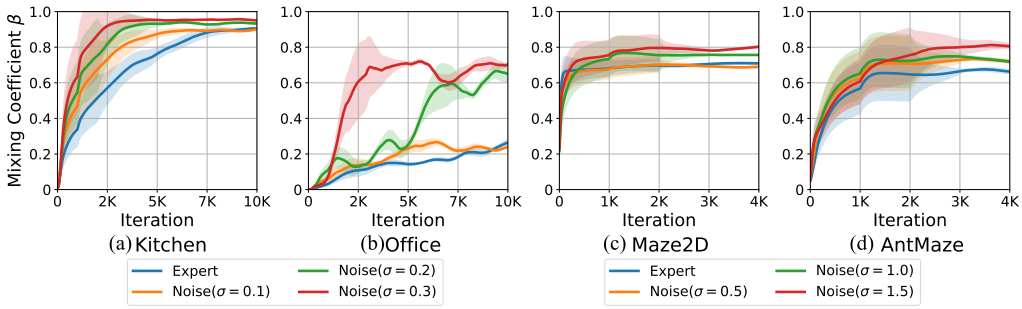

Figure F.1: The evolution of the mixing coefficient β during the meta-train phase

F.2 Additional Visualizations of Refined Skills

Here, we present additional visualization results for SISL in the Kitchen and Maze2D environments. Fig. F.2 illustrates the results in the Kitchen environment ($\sigma = 0.3$) after training is completed. On the left, the t-SNE visualization shows the skill representation $z \sim \pi_{h,\theta}$, while the right side highlights the distribution of skills corresponding to each subtask in the t-SNE map and how these skills solve subtasks over time in the Kitchen environment. In the t-SNE map, clusters of markers with the same shape but different colors indicate that identical subtasks share skills across different tasks. From the results, it is evident that the skills learned using the proposed SISL framework are well-structured, with representations accurately divided according to subtasks. This enables the high-level policy to select appropriate skills for each subtask, effectively solving the tasks. Furthermore, while SiMPL trained on noisy data often succeeds in only one or two subtasks, SISL progressively refines skills even in noisy environments, successfully solving most given subtasks.

Fig. F.3 illustrates how the high-level policy utilizes refined skills obtained at different meta-train iterations (0.5K, 2K, and 4K) during the meta-test phase to solve a task in Maze2D ($\sigma = 1.5$). When using skills trained solely on the offline dataset (meta-train iteration 0.5K), the agent failed to perform adequate exploration at meta-test iteration 0K. Even at meta-test iteration 0.5K, the noise within the skills hindered the agent's ability to converge to the target task. In contrast, after refining the skills at meta-train iteration 2K, the agent successfully explored most of the maze during exploration, except for certain tasks in the upper-left region, and achieved all meta-test tasks by iteration 0.5K. Finally, using skills refined at meta-train iteration 4K, the agent not only explored almost the entire maze at meta-test iteration 0K but also completed all meta-test tasks by iteration 0.5K. Additionally, trajectories generated with refined skills showed significantly reduced deviations and shorter paths compared to those using noisy skills. Overall, the results in Fig. F.3 highlight the importance of SISL's skill refinement process in ensuring robust and efficient performance.

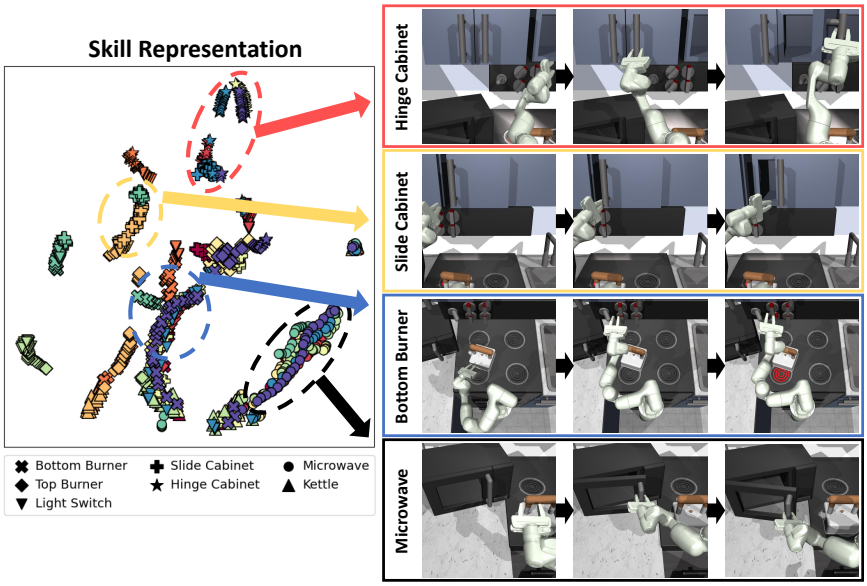

Figure F.2: t-SNE visualization of skill representations (left) and refined skill trajectories for various subtasks (right) in Kitchen ($\sigma = 0.3$). In the skill representation, marker colors denote tasks, while marker shapes indicate subtasks.

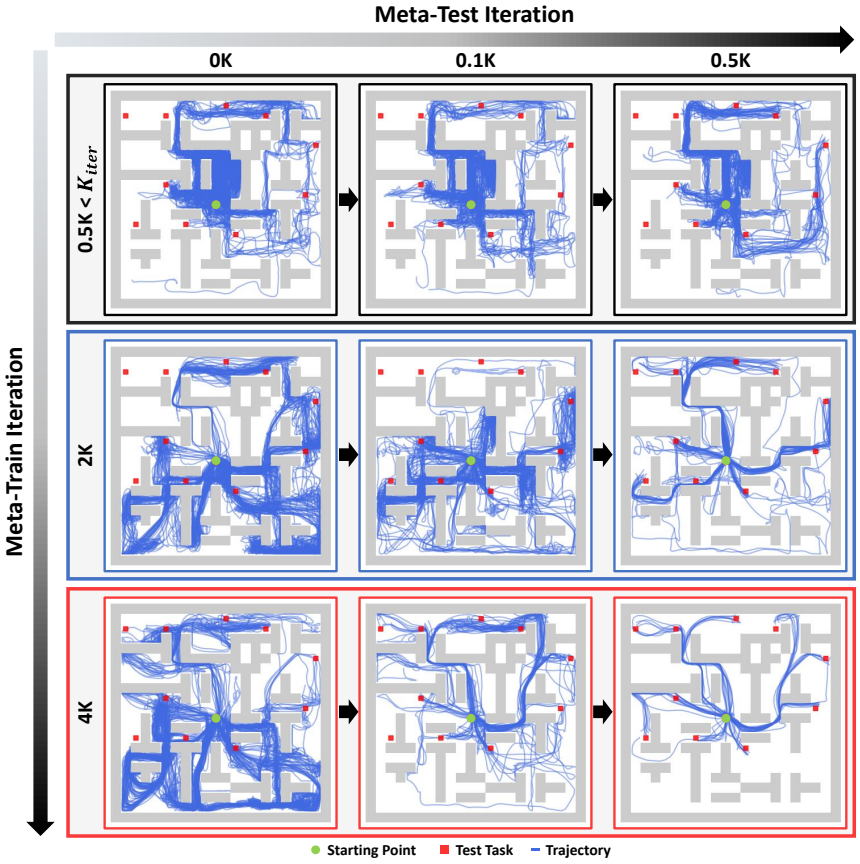

Figure F.3: Illustration of trajectories of refined skills during the meta-test phase in Maze2D ($\sigma = 1.5$), across various training and test iterations.

F.3 Improvement in Task Representation through Skill Refinement

Fig. F.4 illustrates the effect of skill refinement on task representation through t-SNE visualizations of task embeddings $e^{\mathcal{T}} \sim q_e$ in the Kitchen environment ($\sigma = 0.3$), with different tasks represented by distinct colors. In Fig. F.4 (a), the task encoder is trained using fixed skills directly derived from noisy demonstrations. The noisy skills obstruct the encoder's ability to form clear task representations, making task differentiation challenging. This limitation highlights why, in SiMPL, relying on skills learned from noisy datasets can sometimes result in poorer performance compared to SPiRL, which focuses on task-specific skill learning.

Conversely, Fig. F.4 (b) presents the t-SNE visualization when the task encoder is trained during the meta-train phase with refined skills. The improved skills enable the encoder to form more distinct and task-specific representations, facilitating better task discrimination. This improvement allows the high-level policy to differentiate tasks more effectively and select optimal skills for each, thereby enhancing meta-RL performance. These findings demonstrate that the proposed skill refinement not only improves the low-level policy but also significantly enhances the task encoder's ability to represent and distinguish tasks, contributing to overall performance improvements.

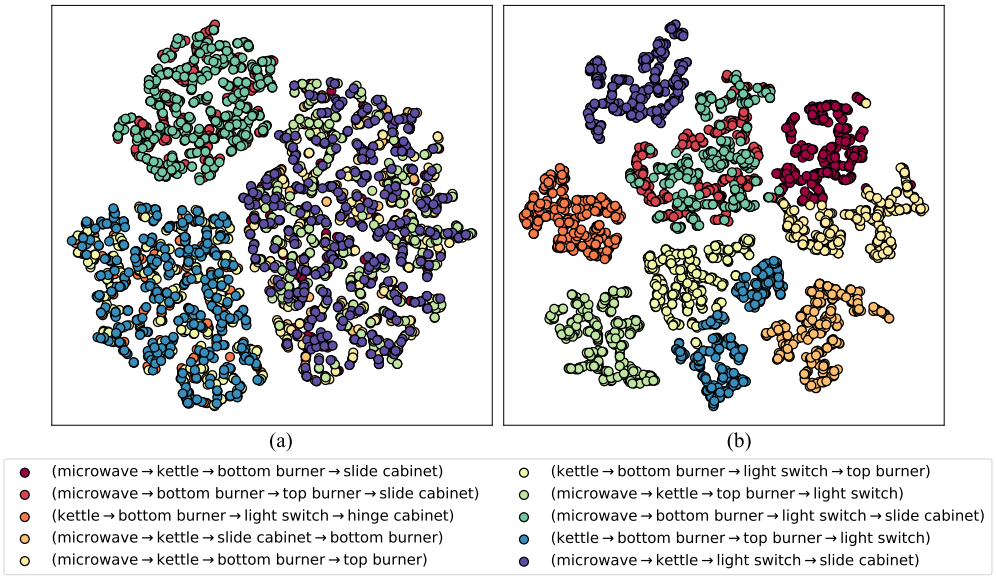

Figure F.4: t-SNE visualization of task representations in the Kitchen environment ($\sigma = 0.3$): (a) Using only the noisy offline dataset, (b) Proposed SISL trained with refined skills

F.4 Stability of Reward Model Learning

Unlike offline-RL, which typically relies on reward-labeled datasets, skill-based RL operates on reward-free offline data. In SISL, only the skills are learned from the noisy offline trajectories, while the reward model and the high-level policy are trained online using clean, noise-free training tasks, as in SiMPL. As shown in Eq. (4), the reward model is trained using transitions sampled from $\mathcal{B}^i_{\text{imp}}$ and $\mathcal{B}^i_{\text{on}}$, which contain only online trajectories collected by interacting with training task i. Since these buffers contain no offline data, the reward model is unaffected by offline noise. To further support this point, we present Table F.1, which shows that the MSE of the reward model remains consistently low across different offline noise settings in the Kitchen environment. These results indicate that the reward model maintains high accuracy and continues to support effective relabeling even when offline skill pretraining is noisy.

Table F.1: MSE of reward model under different noise levels in the Kitchen environment.

	Kitchen(Expert)	Kitchen(σ=0.1)	Kitchen(σ=0.2)	Kitchen(σ=0.3)
MSE	$0.005_{\pm 0.001}$	$0.005_{\pm 0.001}$	$0.004_{\pm 0.001}$	$0.005_{\pm 0.001}$

G Additional Ablation Studies

In this section, we conduct additional ablation studies for Kitchen and Maze2D environments across all noise levels. These studies include component evaluation and SISL's skill refinement-related hyperparameters discussed in Section G.1, prioritization temperature T in Section G.2, the KLD coefficient $\lambda_{\text{imp}}^{\text{kld}}$ for the skill-improvement policy in Section G.3, and additional component evaluation on RND and re-initialization in Section G.4.

G.1 Component Evaluation

Fig. G.1 presents comprehensive results across all noise levels from the component evaluation in Section 5.5. While improvements are modest under conditions with high-quality offline datasets, such as Expert and Noise ($\sigma = 0.1$) for Kitchen, and Expert and Noise ($\sigma = 0.5$) for Maze2D, notable performance gains are still observed. The significant degradation observed in the absence of the skill-improvement policy π_{imp} highlights its crucial role in mitigating minor noise and discovering improved paths. For higher noise levels, such as Noise ($\sigma = 0.2$), Noise ($\sigma = 0.3$) for Kitchen, and Noise ($\sigma = 1.0$), Noise ($\sigma = 1.5$) for Maze2D, excluding the online buffer or skill prioritization via maximum return relabeling ($\mathcal{B}_{\text{on}}$ or $P_{\mathcal{B}_{\text{off}}}$) caused significant performance drops, emphasizing the importance of maximum return relabeling in SISL. Additionally, relying solely on the online buffer without utilizing the offline dataset led to performance deterioration, demonstrating the offline dataset's value in addressing meta-test tasks involving behaviors not available during meta-train. Beyond these specific findings, most trends align with the results discussed in the main text, further validating the effectiveness of SISL's components across different noise levels.

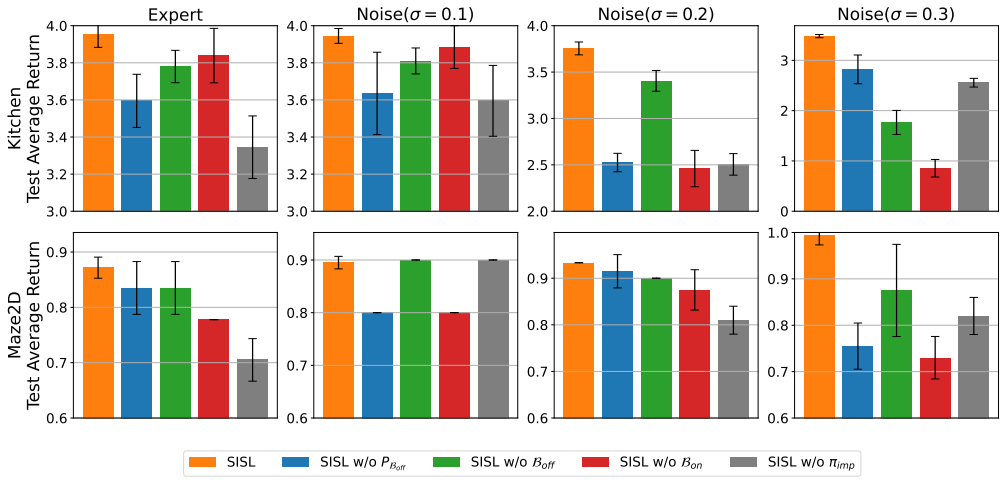

Figure G.1: Component evaluation across all noise levels in Kitchen and Maze2D

G.2 Prioritization Temperature T

The prioritization temperature T regulates the balance between sampling from online and offline buffers. Fig. G.2 shows performance across different noise levels in Kitchen and Maze2D environments as T varies. Low T values lead to excessive sampling from high-return buffers, while high T approximates uniform sampling, diminishing the prioritization effect. Both environments experienced degraded performance at $T = 0.1$ and $T = 2.0$, highlighting the importance of proper tuning. In the Kitchen environment (maximum return = 4), $T = 1.0$ achieved the best performance across all noise levels, whereas in the Maze2D environment (maximum return = 1), $T = 0.5$ was optimal. This difference occurs because environments with lower max returns exhibit smaller gaps between low- and high-return buffers, reducing the effect of prioritization. Based on these findings, we suggest a practical guideline: select T roughly in proportion to the environment's maximum achievable return. This approach offers a principled starting point for tuning T without requiring an extensive hyperparameter sweep, thereby improving usability and reproducibility. Accordingly, we set the best-performing hyperparameter values as defaults for each environment.

G.3 KLD Coefficient $\lambda_{\text{imp}}^{\text{kld}}$

The KLD coefficient $\lambda_{\text{imp}}^{\text{kld}}$ regulates the strength of the KLD term between the skill-improvement policy and the action distribution induced by the prioritized online buffer $\mathcal{B}_{\text{on}}^{i}$ for each task $\mathcal{T}^{i}$. Fig. G.3 illustrates performance variations with $\lambda_{\text{imp}}^{\text{kld}} \in [0, 0.001, 0.002, 0.005]$.

In the Kitchen environment, $\lambda_{\text{imp}}^{\text{kld}} = 0.005$ performed best for Expert and Noise ($\sigma = 0.1$), while $\lambda_{\text{imp}}^{\text{kld}} = 0.002$ and $\lambda_{\text{imp}}^{\text{kld}} = 0.001$ were optimal for Noise ($\sigma = 0.2$) and Noise ($\sigma = 0.3$), respectively. At lower noise levels, the high-level policy benefits from quickly following high-return samples, whereas at higher noise levels, focusing on exploration to discover shorter paths becomes more advantageous. For the Maze2D environment, performance was consistent across $\lambda_{\text{imp}}^{\text{kld}} = 0.001, 0.002$, and 0.005, with only minor variations observed. However, when $\lambda_{\text{imp}}^{\text{kld}} = 0$, removing the KLD term resulted in significant performance degradation across all noise levels in both Kitchen and Maze2D environments. This highlights the necessity of guidance from high-return samples for effectively solving long-horizon tasks. Based on these results, we selected the best-performing hyperparameter values as defaults for each environment.

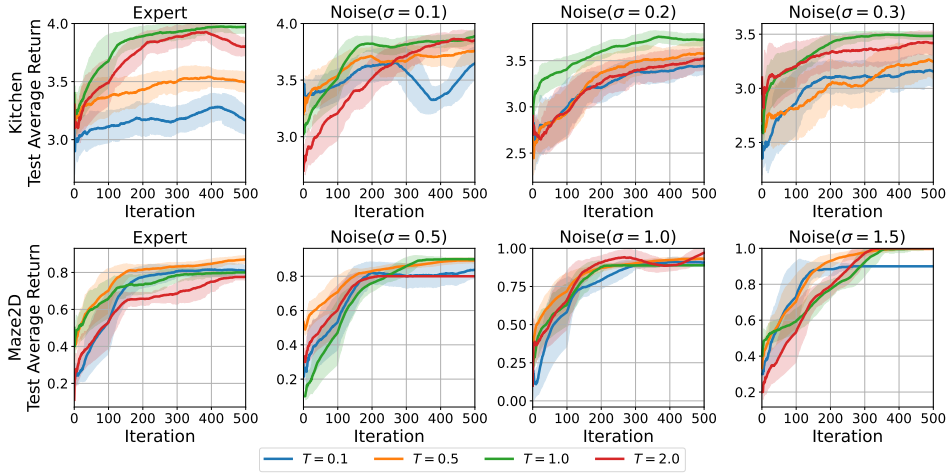

Figure G.2: Impact of the prioritization temperature T across all noise levels in Kitchen and Maze2D

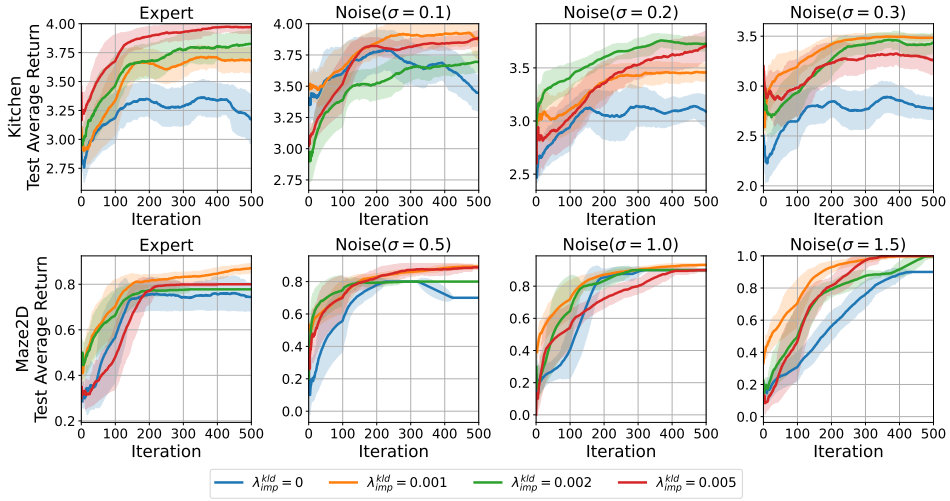

Figure G.3: Impact of the KLD coefficient $\lambda_{\text{imp}}^{\text{kld}}$ across all noise levels in Kitchen and Maze2D

G.4 Additional Component Evaluation

Following the ablation of SISL's core components in Section G.1, we performed additional ablations on the remaining components that could affect performance. These evaluations are conducted in the Kitchen environment using both a Expert and a high-noise condition Noise($\sigma = 0.3$), and the results are shown in Table G.1.

The SISL w/o RND is a variant that excludes RND from skill-improvement policy π_{imp} training and relies solely on SAC. The results show performance degradation compared to full SISL, with especially large drops under high-noise conditions where exploration capability is critical. This suggests that RND encourages exploration toward rare or less frequently visited states, enabling the discovery of more diverse and useful trajectories.

The SISL w/o Re-Initialize refers to a variant that continues training the high-level policy π_h without re-initializing it at each K_{iter} during the meta-training process. In SISL, the skill model is periodically updated every K_{iter} steps, which effectively changes the environment dynamics observed by the high-level policy. Continuing to train the same high-level policy across different skill sets introduces non-stationarity, leading to instability. To address this, we reset both the policy parameters and the buffer at each skill update so that the high-level policy can re-learn from scratch under a new, stable MDP defined by the updated skills. This technique is consistent with practices in continual and safe reinforcement learning, where re-initialization is often used to manage sudden changes in task dynamics (Kim et al., 2023; Kong et al., 2024). To empirically validate this decision, we conducted ablation experiments on high-level policy re-initialization. The results show that removing re-initialization leads to a substantial performance drop, supporting the necessity of this design choice.

Table G.1: Comparison of SISL with/without RND and re-initialization.

Dataset	SISL	SISL w/o RND	SISL w/o Re-Initialize
Kitchen(Expert)	3.97$\pm$0.09	3.90$\pm$0.14	3.11$\pm$0.22
Kitchen($\sigma = 0.3$)	3.48$\pm$0.07	3.14$\pm$0.10	0.41$\pm$0.11